IMPACT OF SOURCE ZONE AND PUMPING WELL ORIENTATION ON DISSOLVED CONTAMINANT DILUTION FACTOR

A Thesis

by

CONNOR TRENT MOORE

Submitted to the Office of Graduate and Professional Studies of
Texas A&M University
in partial fulfillment of the requirements for the degree of

MASTER OF SCIENCE

Chair of Committee,	Hongbin Zhan
Committee Members,	Peter Knappett
	David Sparks
Head of Department,	Michael Pope

May 2017

Major Subject: Geology

ABSTRACT

Capture zone delineation is a simple analytical tool that has been employed in many aspects of hydrological sciences throughout recent history. While using capture zone remediation techniques, the dilution of the source contaminant is closely examined and monitored. The dilution factor is the ratio of the contaminant concentration in the pumped water over the contaminant source concentration (assumed to be constant) in a pump-and-treat setup. It is important because it provides critical information about the fluid dynamics within the aquifer, and shows how much the source has been diluted within the aquifer. The objective of this thesis is to investigate how changing the source geometry and orientation impacts the dilution factor.

The scenario includes an arbitrary line-source length and orientation, fully vertically penetrating well in a homogeneous, horizontally isotropic, confined aquifer. The experiment is set under steady-state conditions. Two analytical models are performed, the first dealing with three subcases consisting of constant source concentrations (cases 1-3), and the second dealing with three subcases cases involving time-dependent source concentrations (cases 4-6). The integrals associated with cases 4-6 are solved in MATLAB using Gaussian quadrature and Gaussian Kronrod integration methods and demonstrate how each of these source types impacts the dilution factor calculation.

After analyzing the results for the first analytical model, the overall conclusion is that the distance between the pumping well and the source is the dominant variable for increasing or decreasing the dilution factor. The source angle and source length also

have an impact on the dilution factor. As these values decrease, so do the dilution factor values. The MATLAB model shows differing trends for both of the integration methods (Gaussian quadrature and Gaussian Kronrod) and the source types influence the dilution factor. The finite source decreases rapidly as the last of the source reaches the well, and then slowly flattens out until there is no longer a concentration in the system. The radioactive source and the Gaussian type source decrease with increasing time measurements. The models can be retrofitted for other source types and different variables to fit differing scenarios. Overall, the results will help with planning for future remediation projects, and these models allow for an initial screening test to be done before more robust, time intensive and expensive models can be put into place.

ACKNOWLEDGEMENTS

I would like to thank Texas A&M University for their support throughout my time here in the Geology & Geophysics department. They have allowed me to shape a career in geosciences, and for that I am grateful. I would also like to thank my advisor, Dr. Hongbin Zhan, for helping me throughout the process of graduate school. This thesis project would have been much more difficult without his guidance and advice. My advisory committee members Dr. Peter Knappett and Dr. David Sparks have been accommodating with any questions along the way as well.

Finally, I would like to thank my friends and family. Throughout my toughest times, they have always stood by my side and encouraged me to be the best person I can possibly be. You have been such a blessing in my life and I cannot thank you enough for everything you do.

CONTRIBUTORS AND FUNDING SOURCES

Contributors

This work was supported by a thesis committee consisting of Dr. Hongbin Zhan, Dr. Peter Knappett, and Dr. David Sparks of the Department of Geology & Geophysics.

All work for the thesis was completed independently by the student.

Funding Sources

There are no outside funding contributions to acknowledge related to the research and compilation of this document.

NOMENCLATURE

a	meant to represent the duration of the source [T]
B	thickness of the confined aquifer [L]
C_0	constant concentration at the source [M/V]
C_w	constant concentration at the extraction well [M/V]
DF	dilution factor
l	half-length of the line source [L]
l_{max}	initial half-length of the line source inside capture zone [L]
Q	pumping rate of the well [L^3/T]
Q_{min}	minimum pumping rate to capture entire source [L^3/T]
Q'	flow discharge per unit depth [L^2/T]
q_0	uniform regional flow specific discharge [L/T]
T_0	represents the travel time from a specific starting point [T]
t	represents the time of measurement of C_w [T]
x_0	distance from the center of the line source to extraction well [L]
y	y coordinate at an arbitrary point along the streamline [L]
y_0	y coordinate at the source endpoint [L]
θ_i	polar angle of a starting point at the source
θ_f	entering angle of a streamline to the extraction well
φ	streamline value passing through source [L^2/T]
σ	standard deviation [T]
ω	decay constant [1/T]

TABLE OF CONTENTS

LIST OF FIGURES

LIST OF TABLES

INTRODUCTION

Groundwater is a precious resource that is used in both urban and rural settings. In the United States, ground water supplies 38% of the population supplied by public water facilities. For rural homeowners, groundwater supplies 97% of the drinking water that isn't delivered by a public service (USGS, 2016). Contamination of these groundwater aquifers is an on-going issue that continually needs to be addressed to maintain a safe and sustainable environment. Leaking storage tanks, landfills, and agriculture related activity is a few examples of sources of contaminants that can infiltrate the ground-water system (Eckhardt and Oaksford, 1988; Miller, 1980; Wollenhaupt et al., 1990). Extraction of the contaminant from a confined or unconfined aquifer can be difficult, and every scenario can require different remediation techniques.

Capture zone delineation is a simple analytical tool that has been employed in many aspects of groundwater science such as designing remediation plans for pump-and-treat scenarios, the well head protection program as used by the US EPA, and various other techniques that have been implemented by the EPA's CERLCA law (Javandel and Tsang, 1986). A capture zone is a region inside the aquifer in which all the groundwater will be eventually captured by a pumping well, assuming steady-state recharge and pumping conditions. When a contaminated source of water is released from, for example a trench, the concentration in pumped water (C_w) does not equal to the source concentration (C_0), or specifically, C_w is smaller than C_0. This is because the extracted water from the pumping well comes from both contaminated groundwater from the source and uncontaminated groundwater outside of the source inside the capture zone.

The ratio of C_w/C_0 is denoted as the dilution factor of the capture zone. To maximize the efficiency of the remediation design and cleanup the contaminant as quickly as possible, one will try to maximize the dilution factor. A lower dilution factor may be desired if a treatment system isn't available and dilution is the best solution.

However, it appears that a host of geometric factors such as source orientation, geometry, and source length influences the dilution factor in various manners. At present, there is no study that is exclusively focused on determining how those different source geometric factors control the dilution factor. Groundwater specialists are continually trying to find faster, more efficient models to help understand the subsurface framework of the aquifer so they are able to do the best job possible at remediating the contaminated site.

OBJECTIVES

The purpose of this Master's thesis is to provide a comprehensive investigation of the dilution factor calculation. The study will utilize two analytical models, the first model consisting of three cases, each one of those cases having four individual subcases. The first model uses an analytical solution for capture zone calculations and these models will be performed in Microsoft Excel. The second model uses MATLAB to solve for the dilution factor. For this analytical model, three different time-dependent source functions will be implemented into a derived streamline function equation. I will discuss the sensitivity of the dilution factor to each of the components that guide remediation design. Furthermore, I will provide a library of type curves describing the relationship between the extraction well concentrations and the source orientation, source geometry, and the distance from the source.

The conditions and parameters for this thesis are purely theoretical, and a simple site assumption is used to explore the effect of important geometric factors on the dilution factor. The findings in this thesis will be influenced by more complex natural conditions such as dispersion, anisotropy and heterogeneity. The scenario includes an arbitrary source length and orientation, fully vertically penetrating well in a homogeneous, horizontally isotropic, confined aquifer. The hydrogeology for the model can be represented by clean, alluvial sand. The study will focus on the steady-state concentration in the pumped water. This is justified because when pumping lasts long enough for a capture zone scenario, that should be the final maximum concentration in the pumping water if neglecting all the dispersive and diffusive effects. Additionally,

the streamline function with the time-dependent sources is integrated and gives an accurate solution for the dilution factor. One of the main goals is to be able to simulate three different source behaviors, and use these results as references for future remediation products.

PREVIOUS WORK

Many capture zone studies have been conducted in the past to help resolve and remedy groundwater contamination incidents. Bear and Jacobs (1965) defined the complex potential theory and superposition to depict how contaminants move throughout an aquifer. Javandel and Tsang (1986) developed a method, which can assist in the determination of the optimum number of pumping wells, and their rates of discharge and locations, such that further degradation of the aquifer is avoided. Streamline function calculations, which are the boundary of a capture zone, were derived from the complex potential theory for single and multiple pumping wells within an aquifer (Javandel and Tsang, 1986). It is essential to understand the importance of capture zone calculation. Overestimation of capture zone boundaries will result in an unnecessarily expensive remediation process, while an underestimation will allow for the contaminants to bypass the well and move down gradient (Bair and Lahm, 1996).

A study concerning capture zone delineation was done in a transient flow system by Bair et al. (1991) which used the Theis equation and the Hantush-Jacob equation to create analytical models. These models simulate different hydraulic properties and aquifer characteristics by incorporating data from locations that can provide geologic/hydraulic properties and pumping rates. They concluded that while analytical models are useful for two-dimensional flow regimes that are not hydro-geologically complex, a numerical model proves to be more robust for areas that are considered to highly heterogeneous. This is because the discretization process involved with a numerical solution provides more accurate solutions than an analytical model (Bair et

al., 1991).

A pump-and-treat scenario will be the setting for this thesis project. The pump-and-treat technique is still the most commonly used strategies for groundwater cleanup projects (Cohen et al., 1997). Shan (1999) and Christ and Goltz (2002) both provide analytical solutions that are based on the complex potential theory and the principle of superposition. These solutions are designed for multiple well pump-and-treat systems. One of the differences between Javandel and Tsang (1986) and Christ and Goltz (2002) and is that Javendel and Tsang created type curves for capture zones using uniform flow rates for all of the wells, while the Christ and Goltz expanded upon these results by implementing varying pumping rates between the wells. It was concluded that the difference between streamline functions is a good indicator of optimal well spacing for a variable pumping rate, multiple well pump-and-treat system (Christ and Goltz (2002).

Many tests have been performed to delineate capture zones to develop the accurate groundwater models. Multiple well tracer tests have been used to simulate aquifer properties, and this technique seems to be the most widely used because of the accuracy and affordability. A few examples of these tests are seen in Ptak et al. (2004), Güven et al. (1986), and Chen and Knox (1997) which make good use of tracers for remediation design.

Heterogeneity can be a big issue when trying to develop a reliable hydrogeologic model. Dispersion effects are one of the main issues when trying to understand the subsurface hydraulic properties of the aquifer. Multiple studies have concluded that dispersion effects and heterogeneity can be disregarded when evaluating non-uniform

flow capture zone problems (Cunningham et al., 2004; Hoopes and Harleman, 1965, 1967). The study for Cunningham (2004) involved a field site consisting of inter-fingering alluvial sediment and gravels. This allows for the capture zone problem to be approximated with confidence because these previous studies prove that these factors have only a minor effect.

Whereas our case analyzes the capture zone for a fully vertically penetrating well within a confined aquifer, multiple studies have performed this for horizontal wells being used for remediation projects. Steward (1999) and Kompani-Zare et al. (2005) both provide analytical solutions for capture zone delineation using horizontal wells. Steward (1999) concluded that a horizontal well that is perpendicular to flow requires a lower pumping rate to capture the contaminant within the upper aquifer boundary. Kompani-Zare et al. (2005) determined, using potential theory, capture zones for a horizontal well that is oriented perpendicular to flow, but with a different well depth and aquifer properties. One of the significant conclusions is that the ultimate capture zone width is smaller for the horizontal well scenario compared to a fully penetrating vertical well. This is caused by the constraining effect of the upper and lower aquifer boundaries.

The travel-time distribution of a source contaminant has also been studied in recent years. The time it takes a fluid particle to flow to a well is considered the capture time. Zhan (1999) derived equations for the analytical calculation of capture time and also verified the results with a numerical model using Visual MODFLOW. The study found that confining boundaries mitigated vertical flow, but augmented horizontal flow

within the aquifer. Zhan and Cao (2000) later expanded on Zhan (1999) to reveal variations in capture time by developing analytical solutions for center and bottom wells in confined aquifers. Analytical solutions were also developed for horizontal wells in aquifers under water reservoirs that serve as constant-head boundaries. The study shows that an aquifer's upper and lower no-flow boundaries play a pivotal role for calculating flow towards a horizontal well. The boundaries will impede vertical flow, while augmenting lateral flow (Zhan and Cao (2000)). Zhan and Sun (2007) then completed a comprehensive investigation over travel-time distribution within a confined aquifer. The study shows how the travel-time distribution of a contaminant responds with variations in the dimensionless source length, dimensionless pumping rate, and varying source types after a certain amount of time. One of the main differences between this thesis and the study done by Zhan and Sun (2007) is that this experiment focuses on the dilution factor, rather than focusing on specific concentrations of a conservative tracer or hypothetical contaminant. The derivations and background scenario of Zhan and Sun (2007) are the precursor for what this thesis will entail.

CONCEPTUAL AND MATHEMATICAL MODELS

The outlined problem is similar to the problem posed in Zhan and Sun (2007). It involves a vertical pumping well that fully penetrates a confined aquifer, and a constant uniform regional flow with a specific discharge q_0 that is moving towards the pumping well. It is assumed that the area within the capture zone is under steady-state conditions. The conservative, continuous contaminant source will initially be treated as a symmetrical line source that is oriented perpendicular to the x-axis. It is treated as a line source for simplification, but the source can also be curved or asymmetrical to the x-axis, which adds to the complexity of the problem. A cross section side view outlining the scenario is shown in Figure 1.

Figure 2 is a two-dimensional schematic diagram showing a line source that is perpendicular to the regional groundwater flow from right to left with a specific discharge of q_0. The pumping well is located at the origin of the Cartesian coordinate system with the x-axis pointing opposite of flow direction and the y-axis parallel to the source. The line source shown in this figure is symmetric in respect to the well, with a length of $2y_0$, and the distance of x_0 from the center of the source to the pumping well. The curve passing through the upper end of the line source (x_0, y_0) and ending in the pumping well represents the outermost streamline of the source. θ_i and θ_f are the polar angle from the source to the end of the well and the entering angle of a streamline to the extraction well, respectively.

The main task for this thesis is to calculate the flow fields for a variety of constant-concentration trench source problems within a confined aquifer. These

variations include changing the source length, inclining angles of the source trench relative to the extraction well, and the symmetry or asymmetry of the source relative to the extraction well. A library of type curves was created to investigate which one of these factors has the most influence on the dilution factor. To calculate the dilution factor, the dimensionless streamline functions and the dimensionless pumping rate of the extraction well was needed. Changing the geometry and orientation of the source impacts the streamline angles created between the pumping well and the origin of the streamline. The streamline angles and the coordinates of the endpoints of the source are both used to calculate the streamline function. The difference between both streamline functions represents the flow rate per unit depth between those two streamlines. The equation (1) for calculating the dilution factor is listed below. The dilution factor is represented by the symbol *DF*, which is the ratio of the concentration of a hypothetical contaminant or a conservative tracer in the pumped water (C_w) versus the constant source concentration (C_0), while the dimensionless streamline function value is φ_D. All the dimensionless terms used are defined in Appendix A, and the subscript "D" represents a dimensionless term. The dimensionless pumping rate for the extraction well is shown by Q_D. Therefore, *DF* can be expressed as (see Appendix A for details of derivation):

$$\boldsymbol{DF = \frac{\varphi_D}{\pi Q_D}} \quad . \qquad \textbf{(1)}$$

The next task involved a MATLAB modeling approach for the time-dependent calculation of the dilution factor. There are three time-dependent source functions that were applied to the streamline function integration to simulate the different source

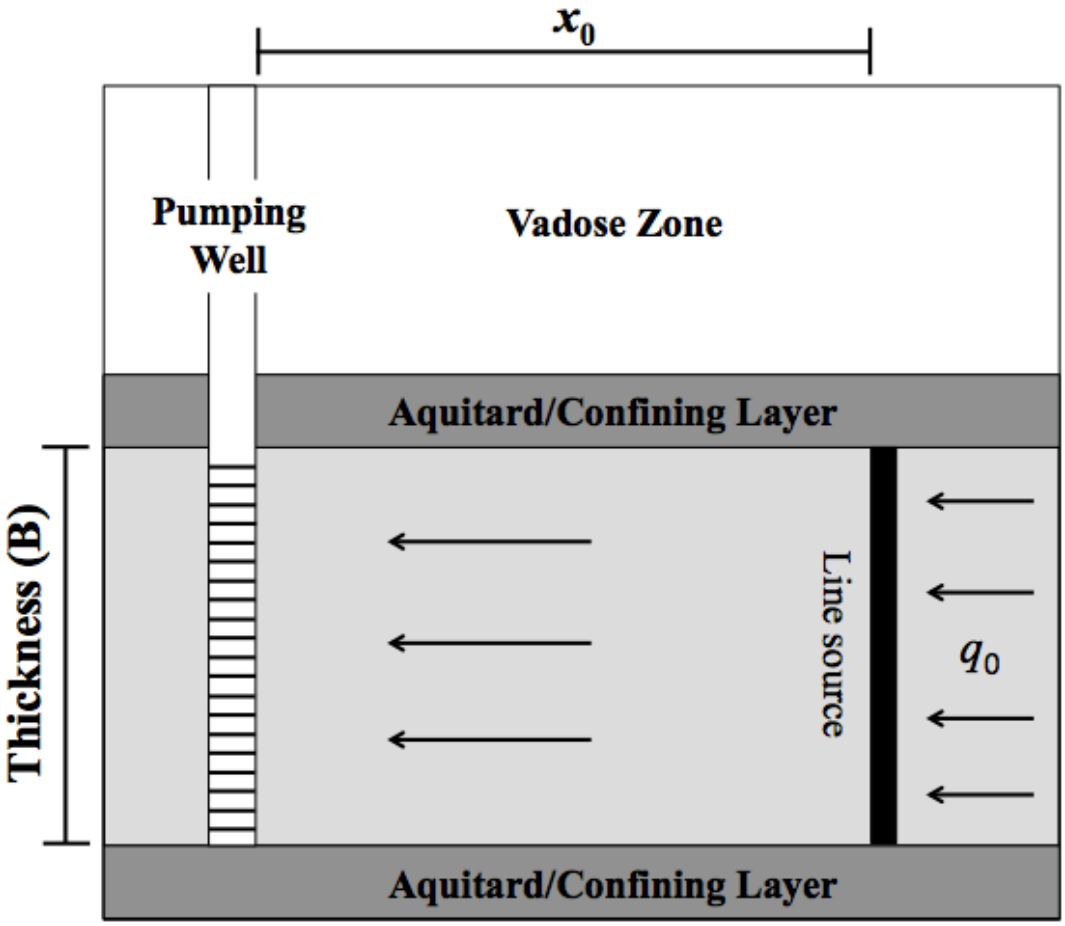

Figure 1 Side-view cross section of the scenario used for this study. A fully penetrating vertical well within a confined aquifer, homogeneous, horizontally isotropic, regional discharge (q_0) flowing from right to left, and a continuous line source perpendicular to the well.

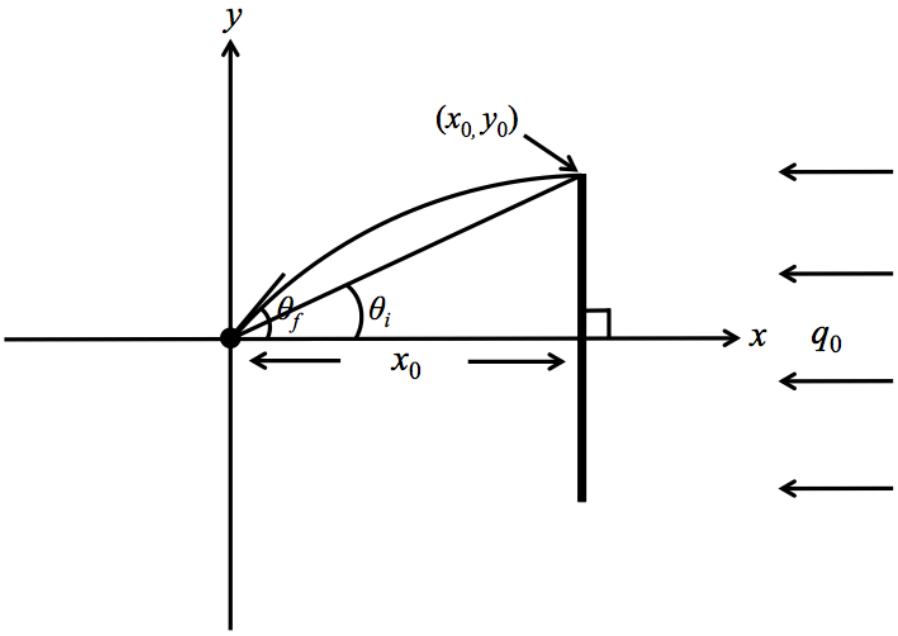

Figure 2 Schematic diagram of a line source that is perpendicular to a regional flow within a capture zone. Assuming a constant pumping rate and constant regional flow. (Modified from Zhan and Sun (2007)).

behaviors that are commonly seen. The integrations were executed in MATLAB because of their difficult and tedious nature to solve analytically.

Constant Concentration Sources (Cases 1-3)

Case 1 – Variable Source Zone Symmetry and Fixed Orientation

For the initial case, the comparison was made between the dilution factor and $\frac{\Delta y}{L}$ ratio, where Δy is how much the endpoints of the source has been shifted to represent an asymmetrical source, and L is the half-length of the line source. During Case 1A, the source length remains fixed; the symmetry of the source will be changed to see how it impacts the dilution factor. The experiment will then be executed again for Case 1B, but the source angle will be changed to 45° while still changing the symmetry of the source for each step. Both of these cases will be done with smaller x_0 values for comparison in Cases 1C and 1D.

Case 2 – Variable Source Zone Orientation and Fixed Symmetry

The next case involves a comparison between the dilution factor and a changing source angle. For Case 2A, the source length remains fixed, symmetrical to the pumping well, and the angle of the line source is changed 11.25° for every step. The center of the line source is located at (x_0, 0). The same experiment is performed again for Case 2B, but the source is asymmetrical while still changing the angle by 11.25°. Figure 3 is located on the following page and is similar to the situation in Figure 2. The line source has a total length of $2y_0$ and is still symmetric in respect to the x-axis, but now the source has been rotated relative to the x-axis. Changing the angle of the source will change the θ_i and θ_f angles, along with changing the x-values for the endpoints of the line source.

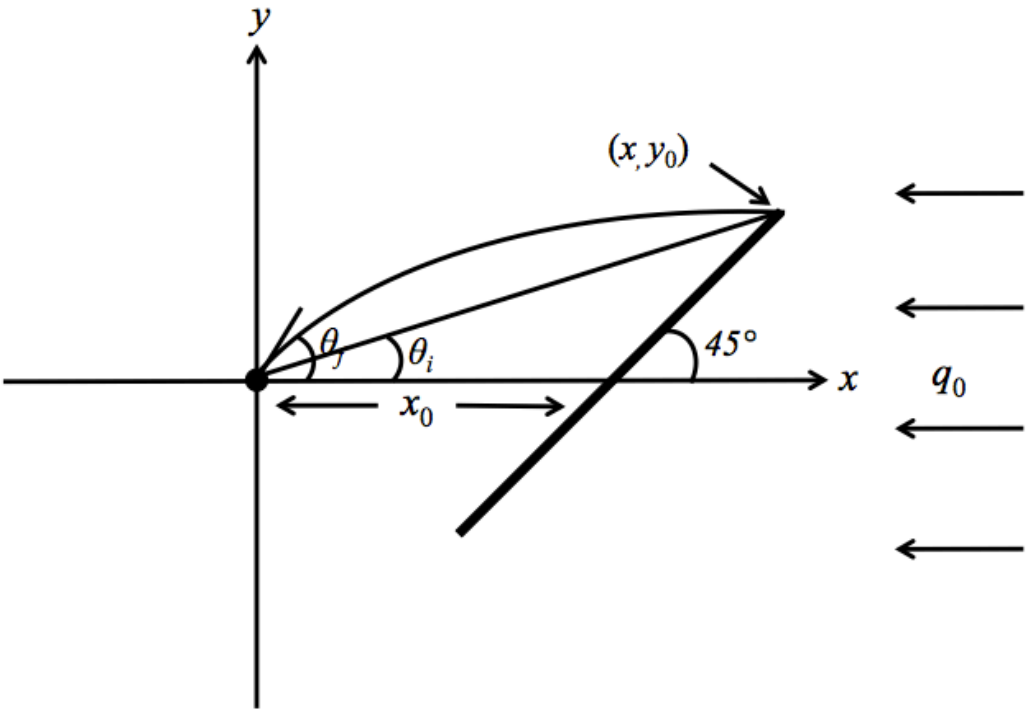

Figure 3 Diagram showing the source has now been rotated 45°, creating new streamline angles and different *y*-coordinates for the endpoints of the line source

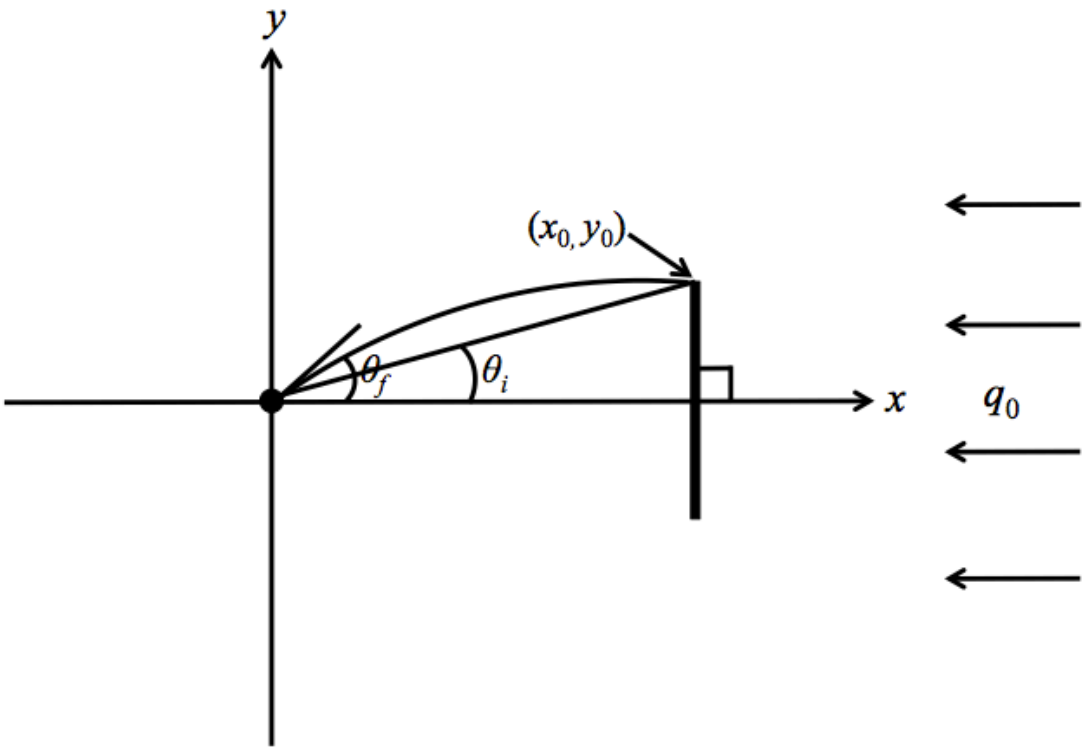

Figure 4 Schematic diagram showing a symmetrical source and a reduced source length to see how this impacts the dilution factor

Case 2C and Case 2D are analogous to the previous cases, only the x_0 value has been reduced.

Case 3 – Variable Source Zone Length and Fixed Symmetry and Orientation

The last analytical model investigates the comparison between the dilution factor and the source length. The comparison was made between the dilution factor and $\frac{y}{x_0}$, where y is the y-value of the endpoint of the source, and x_0 is the distance between the line source and the pumping well.

For Case 3A, the length of the source will incrementally be reduced 10% to see the influence this has on the dilution factor. The experiment is performed again with the same scenario in Case 3B, but with a fixed source angle of 45° to see how this changed angle, combined with a decreasing source length impacts the results. Finally, Case 3C and Case 3D are similar to 3A and 3B but with a reduced x_0. Figure 4 shows the scenario of a perpendicular, symmetrical line source. The streamlines are passing through the source endpoints at (x_0, y_0) but each one has different y_0-values whenever the source length changes. The length of the source is reduced by 10% for each step to see how this will impacts the dilution factor.

Time-Dependent Source Concentrations (Cases 4-6)

The analytical models described above assume steady-state conditions in both the flow field and the source zone concentrations. Under certain circumstances, however, source concentrations may change over time. For example, the source may be excavated after a finite period of time, thus the source is better treated as a step function over a finite duration. The source may also go through a radioactive or biological decay

process, in which case it is better described as an exponentially decaying function with the decay constant determined by the half-life of the source. Given these possible scenarios, the MATLAB model involves three different time-dependent source functions. These functions are as follows.

Case 4 - Step function

$$f(t) = \begin{cases} 1 \ (0 \leq t \leq a) \\ 0 \ (t \geq a) \end{cases}, \quad \textbf{(2)}$$

where *a* is meant to represent the duration of the source [T].

Case 5 - Exponential function

$$f(t) = e^{-\omega t}, \quad \textbf{(3)}$$

where the symbol ω represents the decay constant [1/T].

Case 6 - Gaussian function

$$f(t) = e^{-\frac{t^2}{2\sigma^2}}, \quad \textbf{(4)}$$

where symbol σ represents the duration of the peak of the source [T].

These functions are now implemented into the following cases to represent different source behaviors that are commonly seen in groundwater remediation.

Case 4 – Time Step Function

Solving the travel-time equation and the streamline function (Appendix A) permitted the fourth case of the study. Case 4 deals with a stepwise function, with which a finite source concentration is measured once the streamline function has reached the pumping well until the duration of the source has passed. The function is then added into the streamline equation, and the integration is performed using MATLAB. For this

case, if time t is less than a, then the function is equal to one. The base equation (5) used in MATLAB for each case is listed below.

$$C_W(t) = \frac{C_0}{\pi Q_D} \int_0^{l_D} f[t - T(y_D)] \left[\frac{Q_D}{1+y_D{}^2} + 1\right] dy_D \ , \quad \textbf{(5)}$$

where $C_w(t)$ represents the concentration at the extraction well for that time measurement, and C_0 is the constant concentration of the source contaminant. The symbol l_D is the dimensionless half-length of the line source, and y_D is the dimensionless y-coordinate at the source. The variable t represents the time of measurement of C_w and $T(y_D)$ represents the travel time from a specific starting point at the source with a certain dimensionless y_D (Appendix A). The symbol f represents any of the above-mentioned functions used to describe the time-dependent source.

For this case, the concentration at the extraction well at time t is given by the equation (5) with the details of the derivation given in the Appendix A. Importantly, time t must be greater than the maximum $T(y_D)$, since the late-time behavior of the dilution factor under steady-state conditions is of interest. This is because the late-time behavior of the dilution factor is of most concern from a remediation perspective. Once the concentration at the extraction well is solved, we can now calculate the dilution factor from equation (1) above.

Case 5 – Exponential Decay Function

The next case will have a similar scenario as Case 4. The main difference between Case 4 and Case 5 is the source function. Case 5 will analyze the impacts of having a reactive contaminant within the system. This function input should show a substantially different dilution factor than Case 4. The results are expected to show an

exponential curve behavior that asymptotically flattens out, but after an allotted time measurement, the degradation of the source should begin to decrease the dilution factor. This is important to understand because radioactive waste is a common contaminant found in groundwater systems (Fetter, 1999). The equation (6) for Case 5 is listed below and the symbol ω represents the decay constant describing the rate of decay for the time-dependent source concentration.

$$C_W(t) = \frac{C_0}{\pi Q_D} \int_0^{l_D} e^{-\omega[t-T(y_D)]} \left[\frac{Q_D}{1+{y_D}^2} + 1\right] dy_D \; . \quad (6)$$

Case 6 – Leaking Source Function

The final case involves a Gaussian distribution function that will be applied to the equation to help with understanding a leaking source type. This concentration curve should have a bell shape and will have a more gradual decrease than Case 4. The concentration in the extraction well depends highly upon what the standard deviation value is for the source. The constants within equation (7) will be determined from common groundwater situations and will be slightly varied to see what factor has the biggest impact on the equation. The duration is shown by the symbol σ, which is used to describe the Gaussian shape time-dependent source concentration function. The equation (7) for Case 6 is listed below, with the Gaussian source function.

$$C_W(t) = \frac{C_0}{\pi Q_D} \int_0^{l_D} e^{-\frac{\left(t-T(y_D)\right)^2}{2\sigma^2}} \left[\frac{Q_D}{1+{y_D}^2} + 1\right] dy_D \qquad (7)$$

METHODOLOGY

The methods developed in this project were created in Microsoft Excel for cases 1-3 and MATLAB computer programs for cases 4-6. These programs are user friendly and are sufficient for making the needed calculations for this project. In Table 1, an example of Case 1A is provided with the values and format for the analytical model. The model consists of three analytical cases and their sub-cases that are outlined specifically in the section below. Depending on the changes that were made in each of the cases, this will display different results for the graphs that are created. The constant values used in each case were Q = 187.72 m^3/day, B = 20 m, and q_0 = 0.1 m/d. Table 2 on the following pages is meant to be a helpful guide for summarizing varied parameters in Cases 1-3.

Constant Concentration Sources (Cases 1-3)

Case 1 – Variable Source Zone Symmetry and Fixed Orientation

For Case 1A, the goal of the experiment was to see what the impact of changing the symmetry of the source had relative to the pumping well. The base parameters for the test are the regional discharge q_0, the aquifer thickness (B), the distance between the source and the pumping well (x_0), the y-coordinates for the endpoints of the source contaminants (y_1, y_2), and the half-length of the source (l). The other variables that are shown in the model can all be calculated by using these parameters. The main adjustment in this experiment was changing the y_1 and y_2 coordinates to simulate a change in symmetry for the source. In the program, the coordinates for the initial endpoints of the source are (20 m, 10 m) and (20 m, -10 m). For each subsequent step,

Table 1. Case 1A data showing how each analytical case was setup in Excel.

Case 1A

Q_{min}	Q ($4*Q_{min}$)	Δy	$\Delta y/y$	B (m)
46.93	187.72	0	0	20
52.38	187.72	1	0.1	20
57.97	187.72	2	0.2	20
63.68	187.72	3	0.3	20
69.51	187.72	4	0.4	20
75.46	187.72	5	0.5	20
81.51	187.72	6	0.6	20
87.66	187.72	7	0.7	20
93.90	187.72	8	0.8	20
100.24	187.72	9	0.9	20

l_D	y_1 (m)	y_2 (m)	$\lvert\psi_1 - \psi_2\rvert$	x_0 (m)
0.5	10	10	3.385	20
0.55	11	9	3.383	20
0.6	12	8	3.376	20
0.65	13	7	3.364	20
0.7	14	6	3.348	20
0.75	15	5	3.327	20
0.8	16	4	3.303	20
0.85	17	3	3.275	20
0.9	18	2	3.244	20
0.95	19	1	3.210	20

Streamline Angle 1 (θ_i)	Streamline Angle 2 (θ_i)	q_0 (m/d)	DF
27	27	0.1	0.361
29	24	0.1	0.360
31	22	0.1	0.360
33	19	0.1	0.358
35	17	0.1	0.357
37	14	0.1	0.354
39	11	0.1	0.352
40	9	0.1	0.349
42	6	0.1	0.346
44	3	0.1	0.342

Table 2. Summary of the variables changed in Cases 1-3

Case 1 - Source Symmetry

	Symmetry	Angle	Length	x_0
A	(0,10) - (0,19)	90°	20 m	20 m
B	(0,10) - (0,19)	45°	20 m	20 m
C	(0,10) - (0,19)	45°	20 m	10 m
D	(0,10) - (0,19)	90°	20 m	10 m

Case 2 - Source Angle

	Symmetry	Angle	Length	x_0
A	(0,10)	11.25° - 90°	20 m	20 m
B	(0,15)	11.25° - 90°	20 m	20 m
C	(0,15)	11.25° - 90°	20 m	10 m
D	(0,10)	11.25° - 90°	20 m	10 m

Case 3 - Source Length

	Symmetry	Angle	Length	x_0
A	(0,10) - (0,1)	90°	20 m - 2 m	20 m
B	(0,10) - (0,1)	45°	20 m - 2 m	20 m
C	(0,10) - (0,1)	90°	20 m - 2 m	10 m
D	(0,10) - (0,1)	45°	20 m - 2 m	10 m

the y-coordinates are changed by shifting the line source one meter in the positive y-direction, to represent the change in symmetry of the source. One of the impacts caused by a shift in the endpoints of the source is a need for higher Q_{min} values. Higher change in symmetry for the source. In the program, the coordinates for the initial endpoints of the source are (20 m, 10 m) and (20 m, -10 m). For each subsequent step, the y-coordinates are changed by shifting the line source one meter in the positive y-direction, to represent the change in symmetry of the source. One of the impacts caused by a shift in the endpoints of the source is a need for higher Q_{min} values. Higher pumping rates can have big implications on aquifer drawdown, which is discussed further in the implications section of this thesis.

Case 1B examines the influence of changing the angle of the source to 45° in relation to the x-axis. The same experiment is performed where the symmetry of the source relative to the pumping well is adjusted similarly to Case 1A. It is expected that the dilution factor will be smaller for this experiment, but the goal is to quantify what this difference is between these two cases. The streamline angles and source endpoint coordinates were expected to change significantly, which will make a difference in the dilution factor. The same model is used for this iteration of the experiment, but changing the source angle creates different y-coordinates for the source endpoints. This will subsequently create new streamline angles and change the minimum-pumping rate required to capture the entire source. The streamline angles can be calculated by simple trigonometry between the x_0 and the y_1-coordinate.

Case 1C and Case 1D are similar to Case 1A and 1B, only now the distance between the pumping well and the source is reduced. Expected results for these examples are that the dilution factor should start out higher than their counterparts because of the increase in streamline angles. Theoretically this implies that there would be less fresh water to help dilute the contaminant. Due to the fact the source is now closer to the extraction well, the $Q_{\min}$ would have to increase to encompass the entire line source. This will increase the streamline function angles, creating a smaller distance from the endpoints of the source to the boundaries of the capture zone, resulting in a higher dilution factor. The $\frac{\Delta y}{L}$ ratio should also increase because of the increase in Δy as the source becomes more asymmetrical.

Case 2 – Variable Source Zone Orientation and Fixed Symmetry

Case 2A takes on the premise of adjusting the angle of a fixed source length and constant pumping rate. The main difference between this case and Case 1A and 1B is the systematic change of the source angle while keeping the source symmetry fixed in relation to the extraction well. Calculating the new *y*-coordinates with a different angle will create different dilution factor values in the model. Case 2B utilizes the same methodology as the previous cases, only changing the symmetric source to asymmetric. The *y*-values for both Case 2A and 2D are (0, 10) and (0,-10). To represent an asymmetric source, the *y*-values were shifted to (0,15) and (0,-5) for Case 2B and 2C. These *y*-values remain fixed for each subcase, whereas in Case 1 the *y*-values were changing each step. Case 2C and Case 2D are similar to Case 2A and Case 2B, only now the x_0 value has been minimized to 10 meters in the model. The decrease in x_0

should produce larger streamline angles, therefore creating higher dilution factor values. The decreasing *y*-values are going to influence the dilution factor as the source is rotated.

Case 3 – Variable Source Zone Length and Fixed Symmetry and Orientation

For Case 3A, the approach was taken to create a ratio between the *y*-value of the endpoint of the source (*y*) and the distance between the source and extraction well (x_0). The source will be set at 90° and perpendicular to regional flow. The initial length of the source started at 20 meters and was reduced 10% for each step. As the source becomes smaller, the streamline angles will be reduced. Eventually, the streamline angles for a source that is closer to the well will be equivalent to the streamline angles for a source that is farther away, but larger in size. This is the reason why the *y*-value is normalized by the x_0 value.

Time-Dependent Source Concentrations (Cases 4-6)

The second model deals with a time-dependent source concentration using a MATLAB program to facilitate the computation, which is different to the methodology used in the first analytical model dealing with a constant source concentration. The model uses a symmetrical, perpendicular source relative to the pumping well, with a regional discharge moving from right to left. Each of these cases is performed in MATLAB and the script for each model was either originally written or modified from a previous code (Winckel, 2004). The three cases that were performed in the model had two different approaches that were used. The first uses Gaussian quadrature as the integration technique, which generates a set of abscissas and weights, and the number of nodes determines the number of iterations. The function is integrated using the

calculated abscissas, and these values are then multiplied by their associated weights. The summation of all of the values is the approximation of the definite integral. A program that uses this integration method is shown in a paper by Park and Zhan (2001). The paper also uses another function called Green's function method to simulate contaminant transport for multi-dimensional finite sources in a finite-thickness aquifer. The second uses a built-in integral function in MATLAB, which uses an approach called Gaussian Kronrod quadrature. Gaussian Kronrod quadrature is an extension of Gaussian quadrature designed to estimate error using "Kronrod Points." These points allow for the abscissas to be reused, compared to Gaussian quadrature, which require new abscissas after each calculation. This method is designed to compute high-order estimates by using the previous values (Calvetti et al., 2000). The difference between these two integration methods is considered the approximate error. After these integration methods were performed, a comparison will reveal how the concentration is impacted by the integration method that is used. To find out the necessary number of nodes and weights to use for the integration, the experiment was performed until the number of nodes no longer changes the precision of the calculation. The percent difference between the two models will be assessed to see how reliable they are to one another. These calculations enable the analytical equations to be solved in a quick and concise way. Performing the integration analytically can be tedious and time consuming and thus is the reason why the MATLAB model is a very useful tool.

Case 4 – Time Step Function

For Case 4, the equation developed for the step function source type was implemented into the MATLAB program to generate a solution to the integral. The first integration method uses the Gaussian quadrature method, and the program that was used (see Appendix A) was designed to calculate the proper *x*-values and their associated weights to solve for the integral. For the second calculation, the integral is solved by the Gaussian Kronrod method in MATLAB. Once the parameters are input in the equation, the program is run, and the solution is produced. After the solution for the first integration model is performed, now the second integration method can be used for comparison. A walk-through of how the functions are used in MATLAB is provided in the Appendix B section. Also, the solution for the equation only calculates the concentration in the extraction well. For calculation of the dilution factor, the value given by the program must be divided by the original concentration of the source. Each integration case has a multitude of variables that are constantly adjusted to see the impact that each one has on the dilution factor. For the integration methods, 40 nodes and weights were sufficient enough to make the calculation as precise as possible. In Case 4, the step function source represents a finite source, so as long as measurement of time at C_w (t) is less than the duration of the source (a), the function will be equal to one, and can be treated as a constant source. However, we are interested in the time interval after the source has been removed. So we must now calculate the dilution factor for the constant concentration, and then subtract the dilution factor value for (t-a). This creates a simple function to integrate and solve for the C_w value as it begins to decrease.

Case 5 – Exponential Decay Function

Case 5 has a similar methodology as Case 4, but this case only changes the function for the equation in the model. The function is changed to an exponential decay function to represent a radioactive source type. Making this change within the equation and in the computer code is a relatively simple task and can be quickly executed. The Gaussian quadrature and Gaussian Kronrod integration methods were also used in this case to show how the models contrasted with one another. Within the equation, the decay constant (ω) is another variable that can be adjusted to fit different scenarios as well. The time measurements will be for t = 20 days, t = 40 days, and t = 60 days. The three different decay constants that are used are TCE = 0.05 $days^{-1}$, DCE = 0.03 $days^{-1}$, and VC = 0.02 $days^{-1}$ (Mieles and Zhan (2012).

Case 6 – Leaking Source Function

In Case 6, the method is similar to Cases 4 and 5. The function is exchanged in MATLAB for another exponential function, simulating a Gaussian distribution. The function represents a leaking source type. The standard deviation is shown by the symbol σ and this will be changed between 5, 10, and 30 days to see the impact it has on the dilution factor and the concentration at the well. The time measurements will also be for t = 20 days, t = 40 days, and t = 60 days. An example of how Case 6 is setup in MATLAB is shown in Figure 5. The equation is input into MATLAB, and then the integration can be performed in the command window.

The time interval that is used during each calculation is important for calculating each of the integrations. There are three different scenarios regarding time that can be

addressed. In order for the source concentration to reach the extraction well, the time measurement at C_w (t) needs to be greater that the time it takes the contaminant particle at $y_D = 0$ to reach the extraction well (T). The first time interval occurs before the first contaminant particle has reached the extraction well. During this time, because the contaminant has not reached the well, the C_w will be equal to zero. The next time interval occurs after the contaminant first reaches the extraction well ($y_D = 0$) until the time it takes for the last contaminant particle starting at $y_D = l_D$ to reach the well. This transient interval is complicated and difficult to solve for and is not the focal point of this study. Lastly, the time period that exists after $T(y_D = l_D)$ is another important interval to investigate. The models presented in this thesis are focused on the time interval occurring after the final streamline passing through the end points of the source has reached the pumping well.

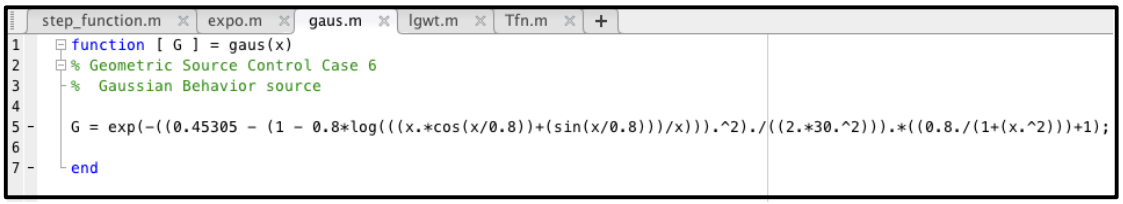

Figure 5 The analytical solution for Case 6 being implemented into MATLAB.

MODEL RESULTS

The results for each case are broken up into two sections. The first section is the observation portion of analyzing the results. This includes value ranges, data trends, and comparing and contrasting subcases to one another. The next section will involve the interpretation of those results to try and delineate why these results are occurring.

Observations

Case 1 – Variable Source Zone Symmetry and Fixed Orientation

The results for each individual sub-case in Case 1 are shown in Figure 10. The graph shows the $\frac{\Delta y}{L}$ ratio on the horizontal axis and the dilution factor on the vertical axis, along with all four of the cases that are conducted in Case 1. Figures 6-9 show the schematic diagram for each individual case showing the geometry and orientation of the source in relation to the pumping well.

For Case 1A, the fixed pumping rate was four times the minimum pumping rate. Since the Case 1A deals with an asymmetrical source, each point that is calculated has different *y*-values. Consequently, this creates differing streamline function angles. The $\frac{\Delta y}{L}$ values for Case 1A ranged from 0 to 0.9 and the dilution factor values ranged from 0.361 to 0.342. The curve demonstrates a small decrease for the dilution factor as the source becomes more asymmetrical. As the $\frac{\Delta y}{L}$ ratio increases, the dilution factor decreases.

Case 1A

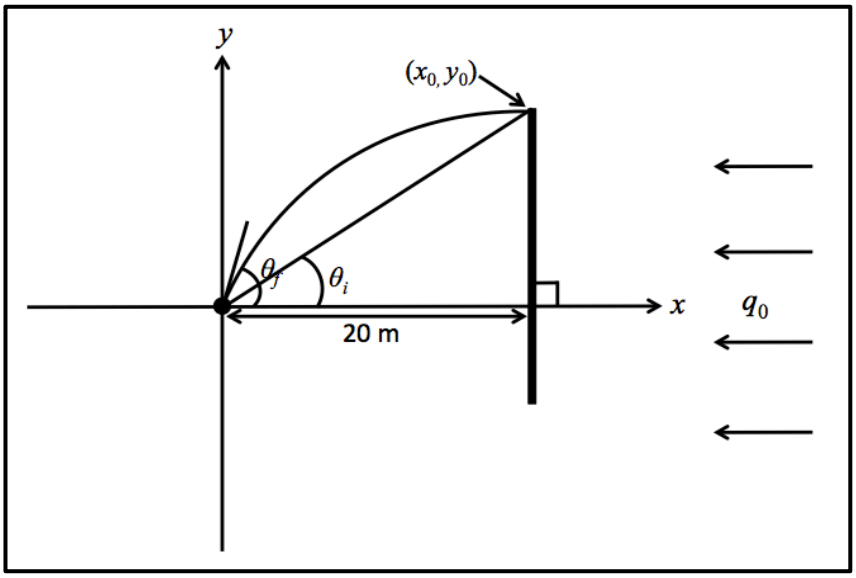

Figure 6 Asymmetrical source at 90° and 20 meters from pumping well

Case 1B

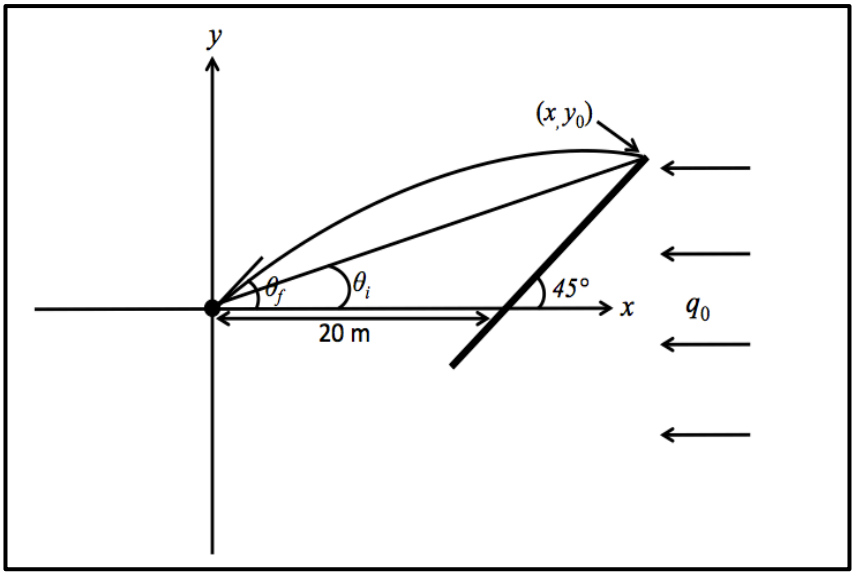

Figure 7 Asymmetrical source at 45° and 20 meters from pumping well

Case 1C

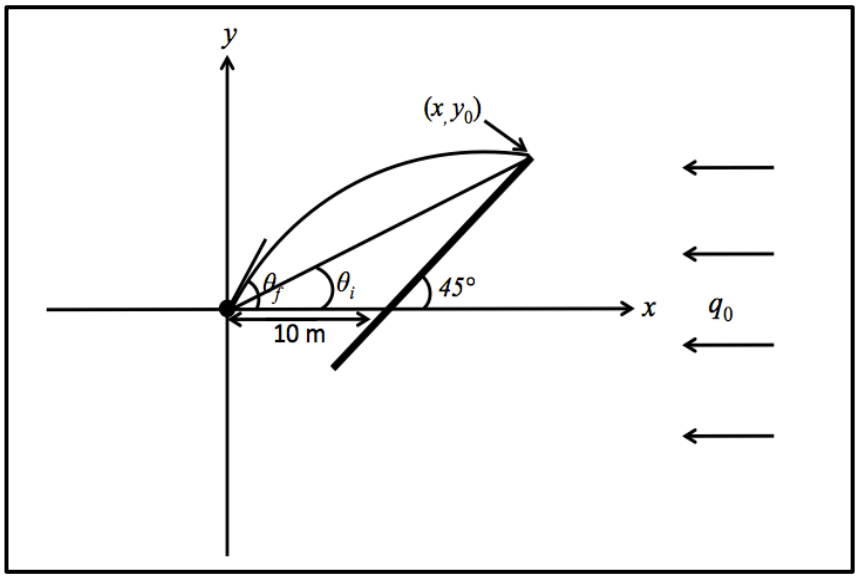

Figure 8 Asymmetrical source at 45° and 10 meters from the pumping well

Case 1D

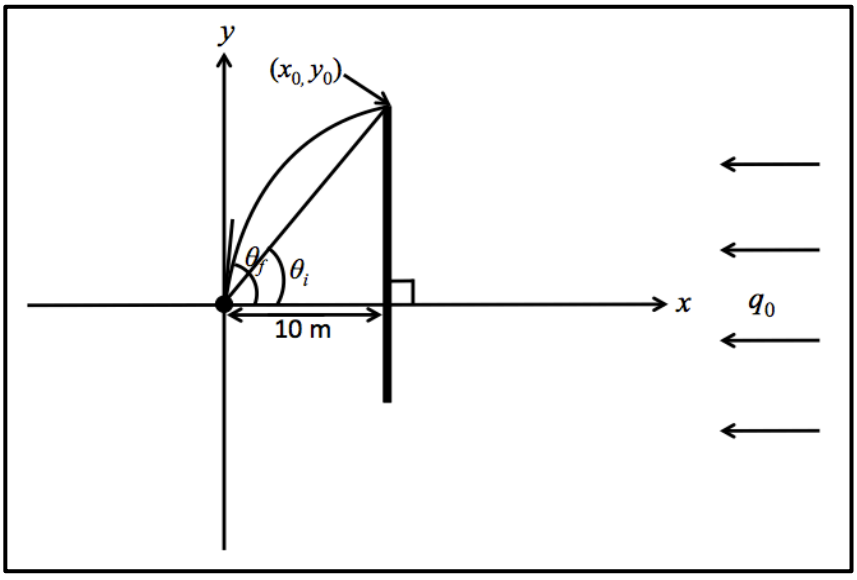

Figure 9 Asymmetrical source at 90° 10 meters from the pumping well

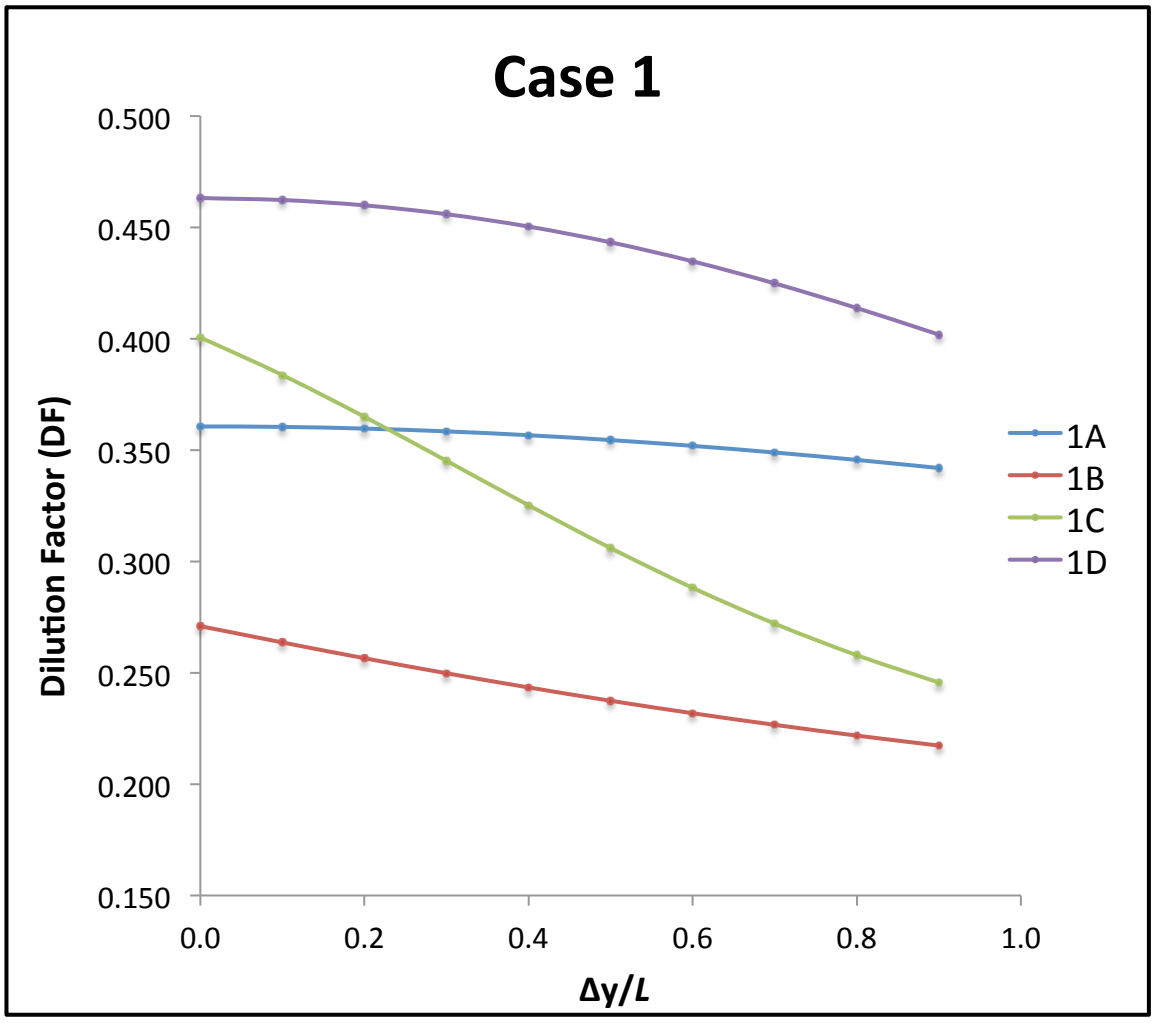

Figure 10 A graph of Case 1 showing the relationship between the Dilution factor (*DF*) and the $\frac{\Delta y}{L}$ ratio.

Case 1B displays similar results to Case 1A, only now the angle for the source has been changed, creating a slightly different outcome. The graph indicates that the dilution factor is initially much smaller whenever the angle of the source is changed to 45°. The values for the dilution factor range from 0.271 to 0.217. The behavior for the curve has a similar shape to Case 1A but the slope is steeper than the previous case.

Case 1C is similar to Case 1B, only now the source is brought closer to the extraction well to see how this influences the dilution factor calculation. The graph indicates that the dilution factors are initially much higher than Case 1B and decreases much faster as the $\frac{\Delta y}{L}$ ratio increases. The average difference for the dilution factor between Case 1C and 1B is 0.08.

Case 1D is the final model that is essentially the same as Case 1A, only the source to pumping well distance was reduced to half of what it was in Case 1A. The results indicate the dilution factor is initially the highest compared to the other cases whenever the distance is shortened. The dilution factor average increase from Case 1A and Case 1D is 0.09.

Case 2 – Variable Source Zone Orientation and Fixed Symmetry

Now that we have established how the symmetry of the source influences the dilution factor, it is now pertinent to understand how the source angle impacts the dilution factor within the capture zone. The main differences between these sub-cases within Case 2 are the symmetry of the source, and the distance between the source and the extraction well. Figure 15 shows the results for Case 2. The source angle is on the horizontal axis, and the dilution factor is shown on the vertical axis. The source angles

Case 2A

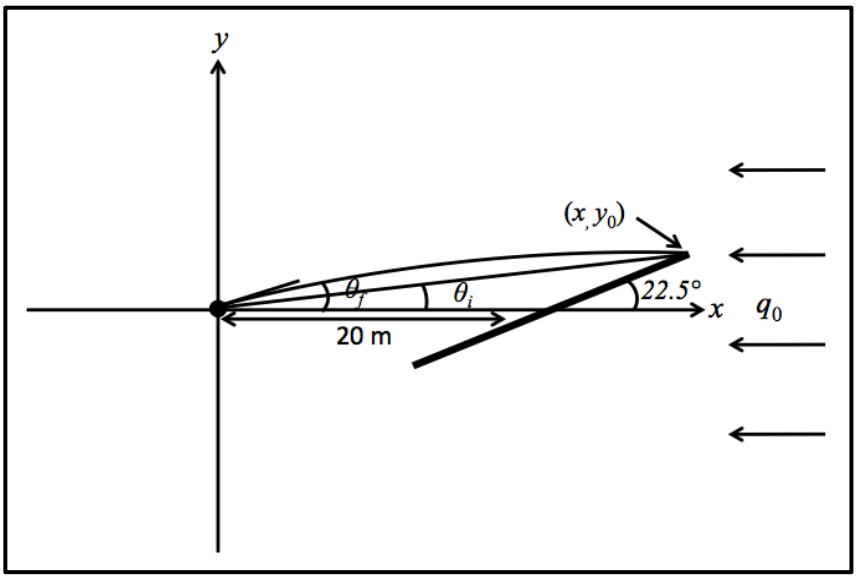

Figure 11 Symmetrical source with decreasing angle, and 20 meters from pumping well

Case 2B

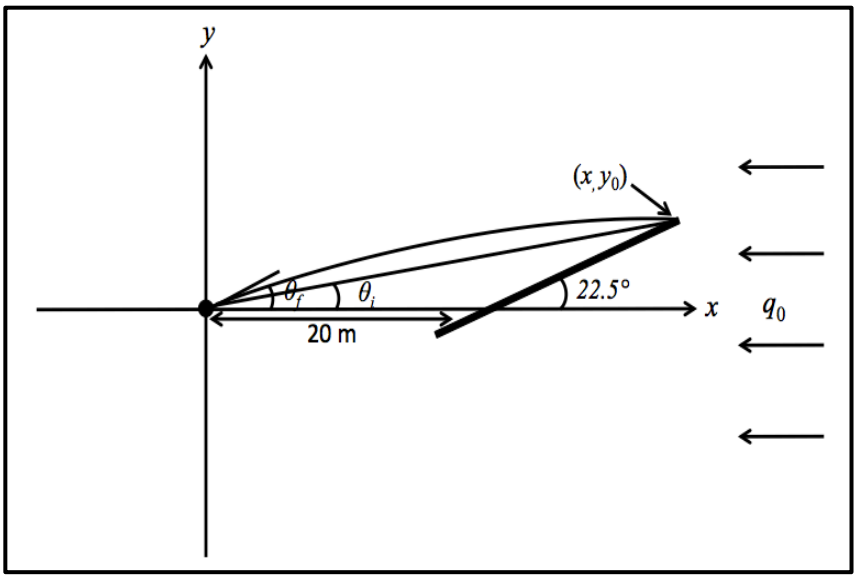

Figure 12 Asymmetrical source with decreasing angle and x_0 = 20 meters

Case 2C

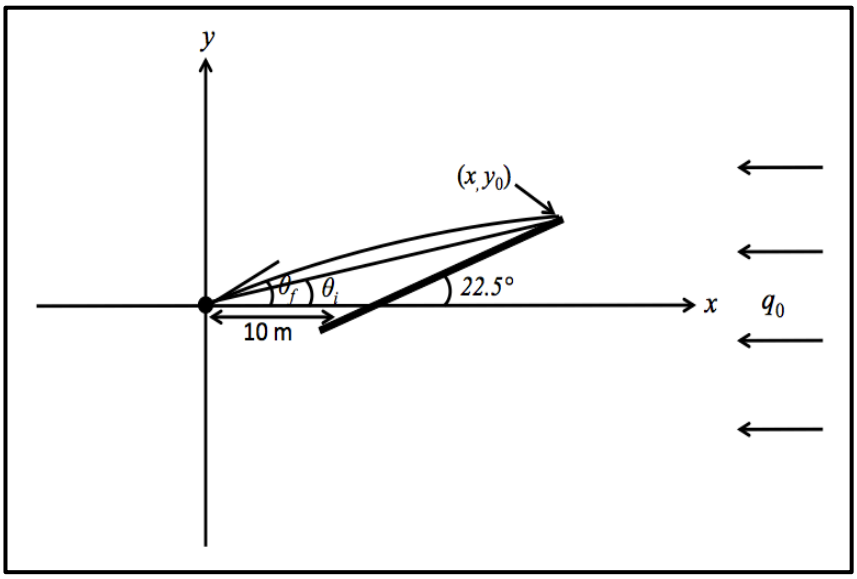

Figure 13 Asymmetrical source with decreasing angle and x_0 = 10 meters

Case 2D

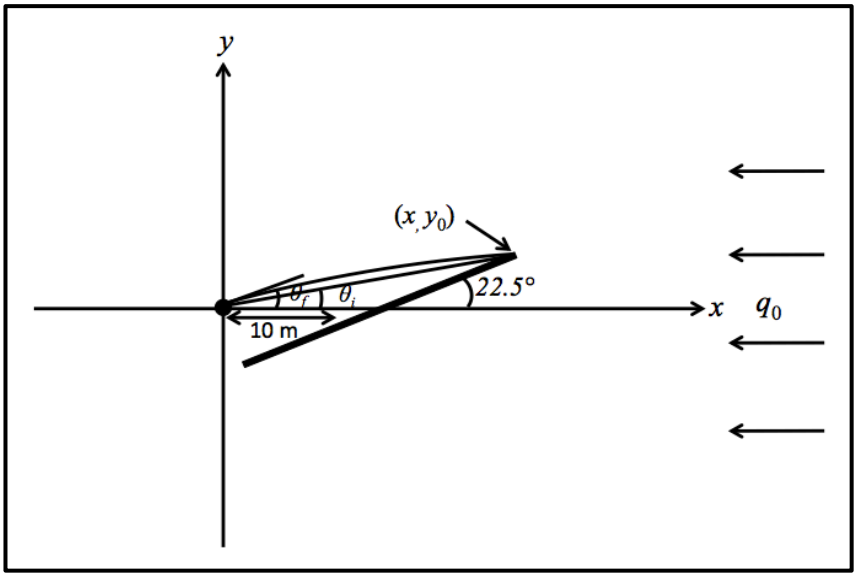

Figure 14 Symmetrical source with decreasing angle and x_0 = 10 meters

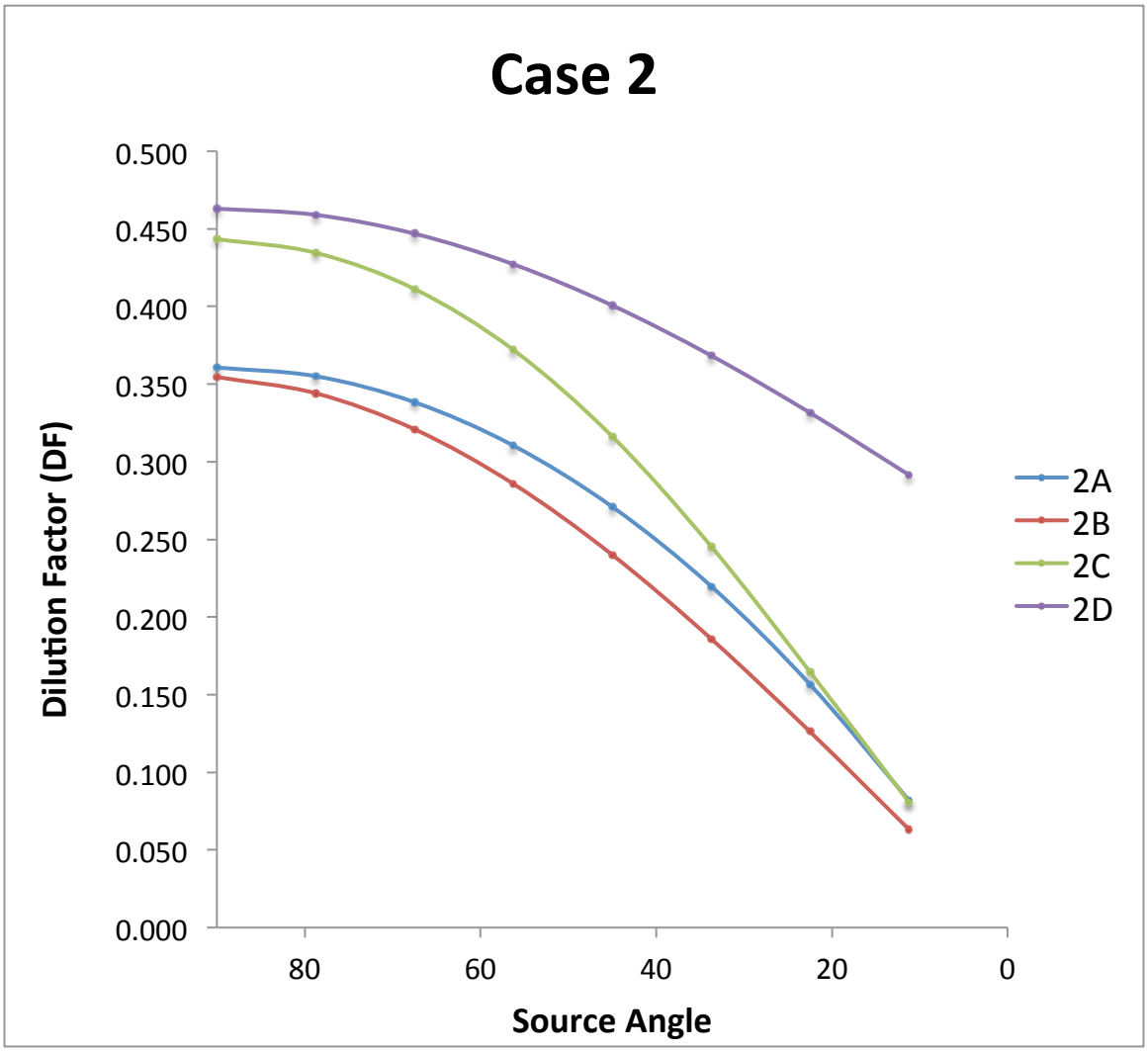

Figure 15 A graph of Case 2 showing the relationship between the Dilution factor (*DF*) and the source angle

on the horizontal axis decrease moving from left to right. The schematic diagrams for the scenario in Case 2A-2D are show in Figures 11-14.

Case 2A involves a symmetrical source, with a constant pumping rate. For each step in the experiment, the source angle is incrementally decreased by 11.25°, starting with 90°. The dilution factor ranges from 0.361 to 0.082 and begins to the decrease as the source angle decreases. The rate of decline for the curve is smaller for higher angles and begins to exponentially increase as the source angles become smaller.

Case 2B is the asymmetrical version of Case 2A and behaves very similarly. With a dilution factor ranging between 0.356 and 0.063, the graph shows that the asymmetrical source generates smaller dilution factors than the symmetrical source. It is reasonable to say that changing the symmetry of the source influences the dilution factor when doing a comparison between the source angles. The most significant difference between Case 2A and Case 2B are when the source angle reaches 56.25°, 45°, 33.75°, and 22.5° with the largest difference being at 33.75° at 0.034.

Case 2C is comparable to Case 2B, only now the distance between the pumping well and the source has been reduced to 10 meters. The source angle is incrementally decreased, similarly to Case 2B. The change in distance creates a dramatic increase in the dilution factor values. The values for the dilution factor range from 0.443 to 0.081 and they display similar curve shapes as Cases 2A and 2B. The curve begins decreasing at a higher rate when the source angle decreases. The dilution factor values converge to zero like the previous cases.

Finally, Case 2D is the last representation of source angle comparison. Diminishing the distance between the source and extraction well is the main difference between Case 2D and Case 2A. The relationship between these two cases is different compared to the Case 2B and Case 2C observation. The curve has a smaller rate of decline compared to Case 2A and the dilution factors are initially larger. The differences between the two curves continue to become larger as the angles get smaller. The curve does not converge to zero like Cases 2A, 2B, and 2C.

Case 3 – Variable Source Zone Length and Fixed Symmetry and Orientation

During Case 3, instead of the investigating the source angle, now the dilution factor is contrasted against the $\frac{y}{x_0}$ ratio. The source length is minimized two meters for each step. The dilution factor is influenced by the increase in source length while keeping a constant pumping rate throughout the experiment. Figure 20 represents the data for experiment done for Case 3. The dilution factor is on the vertical axis and the $\frac{y}{x_0}$ ratio is on the horizontal axis. Figures 16-19 are the schematic diagrams showing the geometry and orientation of the line source relative to the pumping well.

Case 3A is the first experiment for this model. The data shows a nearly linear increase of dilution factor values for this particular case, appearing more linear with the source length being smaller. This is because when the source is smaller, the streamlines that are created become more horizontal. As the streamlines become more horizontal, the dilution factor values will create more of a linear behavior. The results show as the $\frac{y}{x_0}$ ratio begins to increase, the dilution factor begins to increase. The values for the

Case 3A

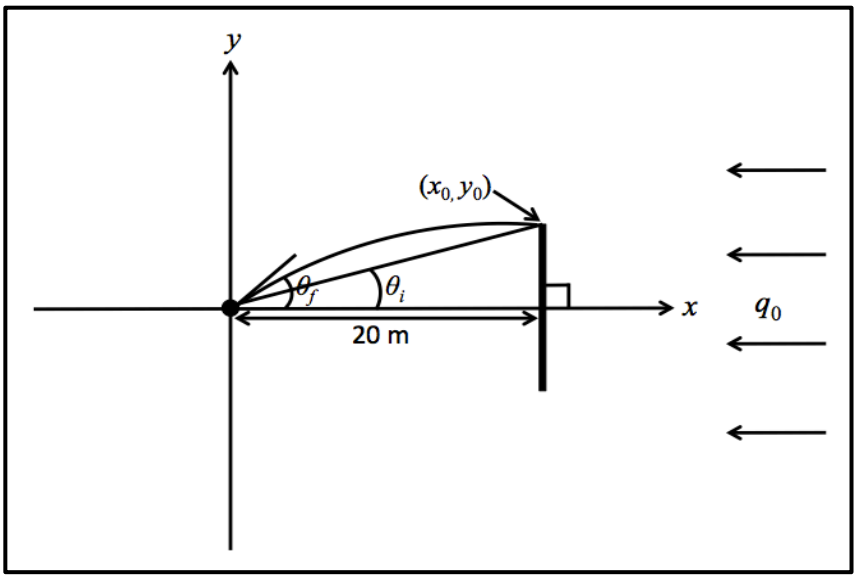

Figure 16 Symmetrical source, 90° and reducing length. x_0 = 20 meters

Case 3B

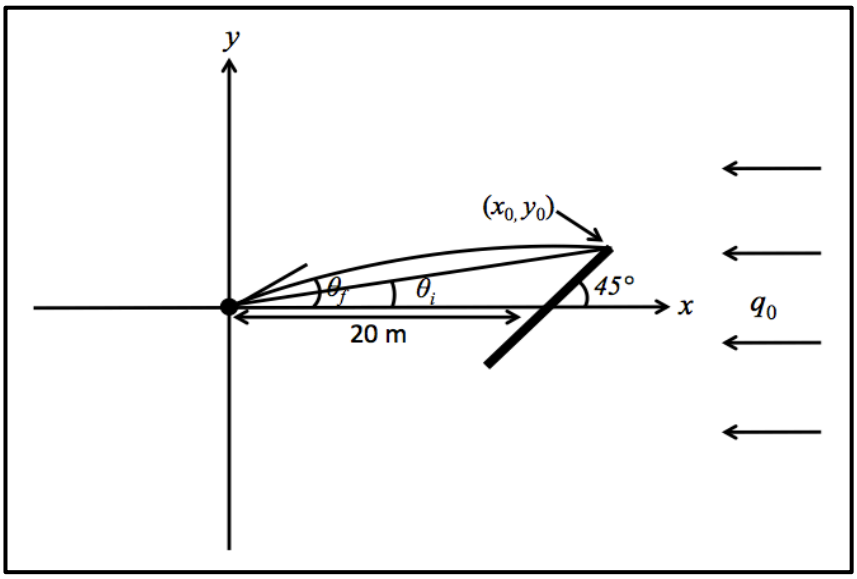

Figure 17 Symmetrical source, 45° and reducing length. x_0 = 20 meters

Case 3C

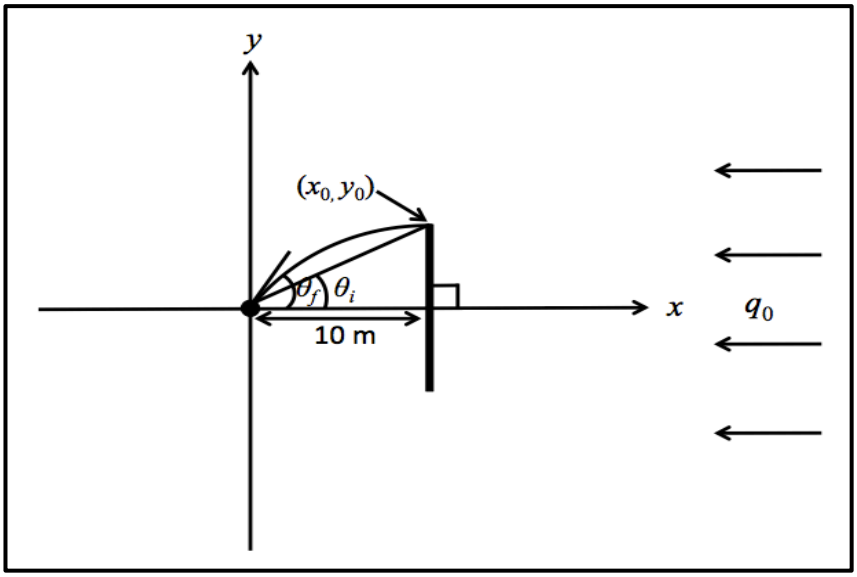

Figure 18 Symmetrical source, 90° and reducing length. x_0 = 10 meters

Case 3D

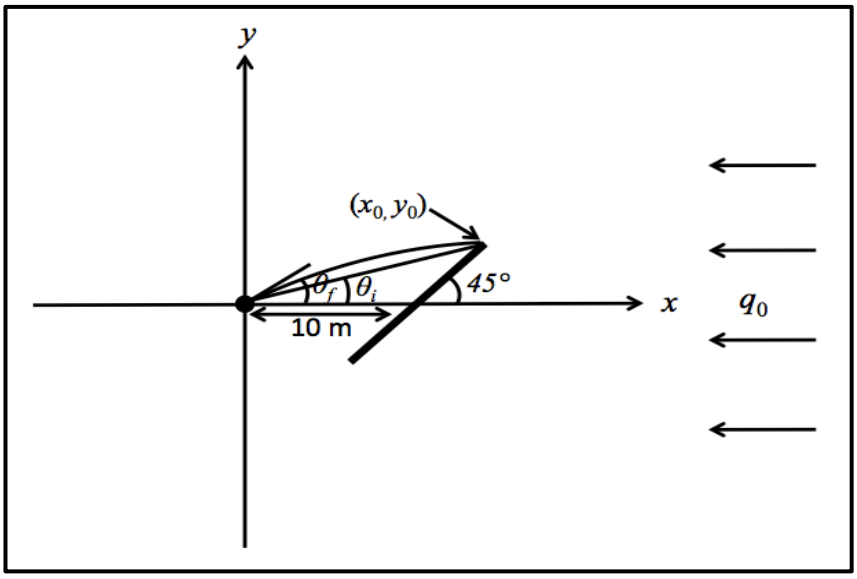

Figure 19 Symmetrical source, 45° and reducing length. x_0 = 10 meters

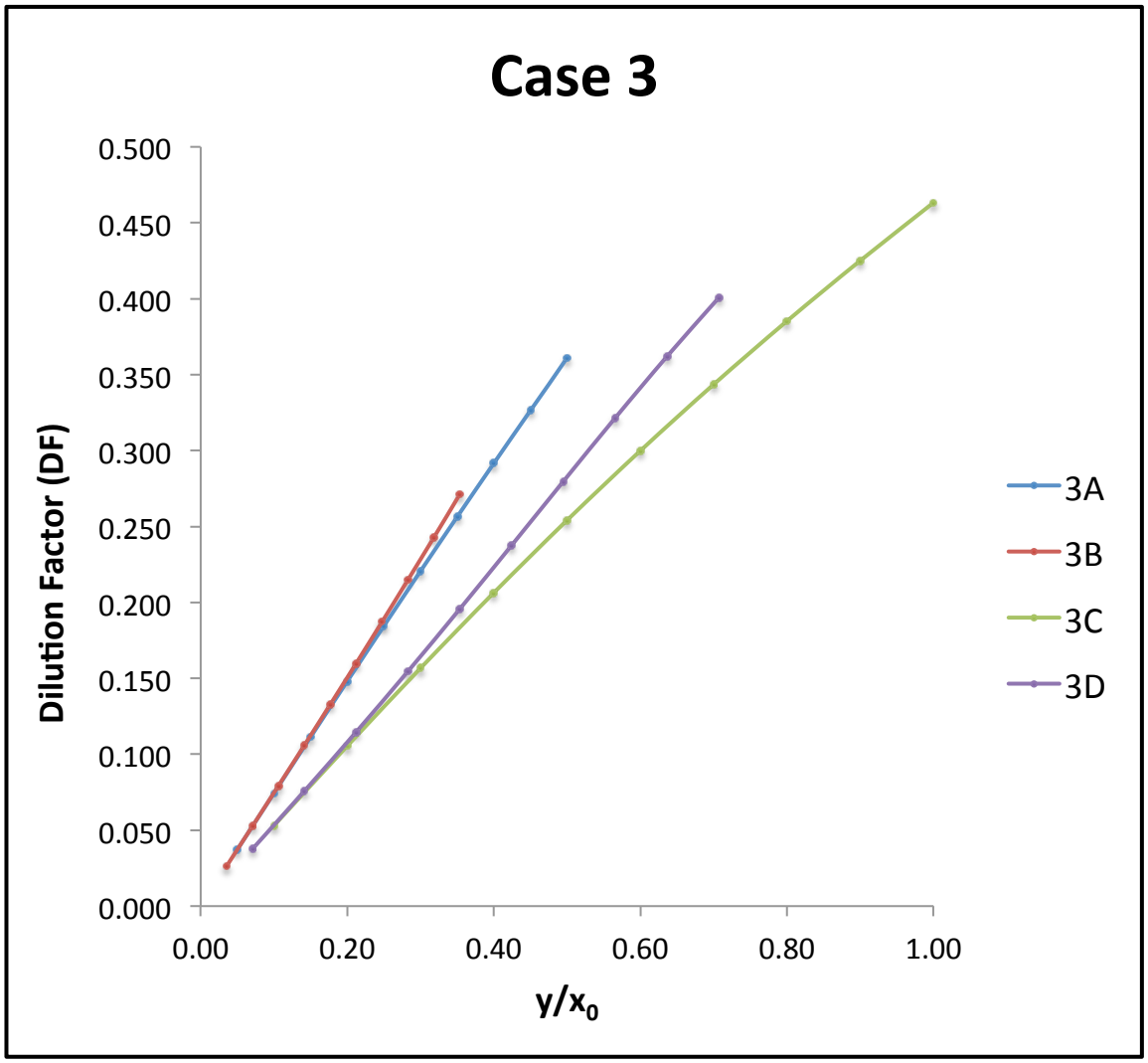

Figure 20 A graph of Case 3 showing the relationship between the Dilution factor (*DF*) and the $\frac{y}{x_0}$ ratio.

maximum and minimum are 0.36 and 0.037, respectively. An increase in the length of the source will create an increasing dilution factor, and the slope is determined by the source angle and the x_0 value.

Case 3B shows a trend that is nearly analogous to Case 3A, only now the source angle has been changed to a 45°. The shape of the curve is very close to being linear, with a steeper slope compared to Case 3A. The initial dilution factor values are considerably smaller than the previous case. The maximum is 0.27 and the minimum is 0.026.

Case 3C shows the highest dilution factor values for any case in this model. The decrease in x_0 creates a much higher dilution factor than Case 3A. The maximum and minimum for the dilution factor range from 0.46 to 0.053, respectively. Case 3D displays the same results, only with a steeper slope and higher dilution factor values than Case 3B. All of the cases converge to zero as the $\frac{y}{x_0}$ ratio approaches zero.

Case 4 – Time Step Function

Now we will look at the results of the integration methods for calculating the analytical solutions that were derived from the time-dependent streamline function equations. With the given variables for this case, both integration methods computed the same result, implying no estimated error for the C_w value. The results for Case 4 are listed below in Table 3, with the duration of the time source (a) being equal to 20 days.

Table 3 The results for Case 4 for a finite source showing both integration methods. The Gaussian quadrature weight function is represented by lgwt. The Gaussian Kronrod method is represented by quadgk. The duration of the source is a = 20 days.

Case 4

***t* (days)**	**lgwt**	***DF***
34 days	0.87092	0.346527
35 days	0.43663	0.17280
36 days	0.61778	0.10072
37 days	0.75082	0.04778
38 days	0.85892	0.00477

***t* (days)**	**quadgk**	***DF***
34 days	0.87092	0.346527
35 days	0.43663	0.17280
36 days	0.61778	0.10072
37 days	0.75082	0.04778
38 days	0.85892	0.00477

Case 5 – Exponential Decay Function

For Case 5, the function is meant to represent an exponentially decaying source contaminant, with the ω changing from 0.05, 0.03, and 0.02 days^{-1}. Each one of the decay constant values was taken from Mieles and Zhan (2012) for three different source types to see how different sources decay rates will influence the dilution factor. Table 4 is shown below, and represents the results for Case 5 with varying decay constants ω, changing time measurements, multiple integration methods, and the dilution factor. The time measurements were changed to see how the increase in time changes the dilution factor. The results shown in Table 4 indicate that for the time measurement at C_w being 20 days, the dilution factor trend is different for the two integration methods. The two methods produced values that differed by a few hundredths from one another. The percent difference between the integration methods changed from 3.9% to 1.5% as the decay constant decreased from 0.05 to 0.02 days^{-1}. The results show that for t = 20 days, the dilution factor has slightly increased as the decay constant decreased for the Gauss-Kronrod method. Conversely, the dilution factor decreases when the decay constant decreases for the Gaussian quadrature method. For t = 40 days the dilution factor continues to become smaller than the dilution factors at previous time measurements for both methods. The dilution factor increases as the decay constant decreases for the Gauss Kronrod method, but the Gauss Quadrature continues to show the opposite trend. Finally, for t = 60 days, both integration methods show increasing dilution factors for decreasing decay constants. Overall, the trend in the data shows a decreasing dilution factor as the time measurement becomes larger. The Gaussian quadrature integration

Table 4 The results for Case 5 for both integration methods and various decay constant values (ω). The Gaussian quadrature weight function is represented by lgwt. The Gaussian Kronrod method is represented by quadgk.

Case 5

ω (decay constant)	***t* = (l_D = 0.5)**	**lgwt**	***DF***
0.05 days^{-1}	20 days	0.903	0.359
0.03 days^{-1}	20 days	0.890	0.354
0.02 days^{-1}	20 days	0.883	0.351
		quadgk	***DF***
0.05 days^{-1}	20 days	0.868	0.345
0.03 days^{-1}	20 days	0.869	0.346
0.02 days^{-1}	20 days	0.870	0.346
ω (decay constant)	***t* = (l_D = 0.5)**	**lgwt**	***DF***
0.05 days^{-1}	40 days	0.880	0.350
0.03 days^{-1}	40 days	0.876	0.349
0.02 days^{-1}	40 days	0.875	0.348
		quadgk	***DF***
0.05 days^{-1}	40 days	0.846	0.337
0.03 days^{-1}	40 days	0.856	0.341
0.02 days^{-1}	40 days	0.861	0.343
ω (decay constant)	***t* = (l_D = 0.5)**	**lgwt**	***DF***
0.05 days^{-1}	60 days	0.859	0.342
0.03 days^{-1}	60 days	0.863	0.344
0.02 days^{-1}	60 days	0.866	0.344
		quadgk	***DF***
0.05 days^{-1}	60 days	0.825	0.328
0.03 days^{-1}	60 days	0.843	0.336
0.02 days^{-1}	60 days	0.852	0.339

method showed higher values compared to the Gaussian Kronrod quadrature method throughout the model.

Case 6 – Leaking Source Function

For Case 6, the source function is now representing a source with a Gaussian shaped distribution. The standard deviation and the time measurement are the main variables changed throughout the experiment. The calculated values for the time interval greater than $T(y_D=l_D)$ are shown for each integration method. The values only vary by a few thousandths for t = 20 days, so the difference is less than 1% for the three standard deviations. As the standard deviation values increase, the dilution factor remains the largest. For t = 40 days and t = 60 days, the dilution factor values decrease as the standard deviation becomes smaller. The model shows that as the time measurements become larger, the dilution factor decreases depending on the standard deviation value. For σ = 30 days, it took a longer time measurement for the dilution factor to decrease significantly compared to σ = 10 days and σ = 5 days. The percent difference between the integration methods increased with smaller standard deviations, but overall remained somewhat constant as the time measurement increased. The results for Case 6 are shown in Table 5 on the following page. The table includes the standard deviation σ, the three different time measurements, both integration method results, and finally the dilution factor.

Table 5 The results for Case 6 for both integration methods and various standard deviations (σ). The Gaussian quadrature weight function is represented by lgwt. The Gaussian Kronrod method is represented by quadgk.

Case 6

σ	***t* = (l_D = 0.5)**	**lgwt**	***DF***
5 days	20 days	0.853	0.339
10 days	20 days	0.866	0.345
30 days	20 days	0.870	0.346
		quadgk	***DF***
5 days	20 days	0.871	0.346
10 days	20 days	0.871	0.347
30 days	20 days	0.871	0.347

σ	***t* = (l_D = 0.5)**	**lgwt**	***DF***
5 days	40 days	0.860	0.342
10 days	40 days	0.868	0.345
30 days	40 days	0.871	0.346
		quadgk	***DF***
5 days	40 days	0.865	0.344
10 days	40 days	0.869	0.346
30 days	40 days	0.871	0.346

σ	***t* = (l_D = 0.5)**	**lgwt**	***DF***
5 days	60 days	0.859	0.342
10 days	60 days	0.868	0.345
30 days	60 days	0.871	0.346
		quadgk	***DF***
5 days	60 days	0.851	0.339
10 days	60 days	0.866	0.345
30 days	60 days	0.870	0.346

Analysis of Results

The following section is devoted to understanding each case and giving some of the reasons why the data is generating the types of trends and values that are seen in the graphs.

Case 1 – Variable Source Zone Symmetry and Fixed Orientation

The results that occurred in Case 1 are predictable and behaved expectedly. All of the sub-cases used an asymmetrical source in the model, but Case 1D exhibits the highest dilution factors because the source is perpendicular to the pumping well. Since the source in Case 1D is closer to the extraction well, an increase in $Q_{\min}$ values is required in order to capture the entirety of the source. The uncontaminated zone becomes much smaller whenever the source is brought closer to the well, mitigating dilution within the pumping well. The closer the source angle is to 90°, the higher the dilution factor will initially be. The x_0 value is the dominant factor over orientation because Case 1C has a much higher initial dilution factor, even though the source angle is 45°. Streamline angles are much higher whenever the source has been brought closer to the pumping well. These higher angles create an increase in the difference between the streamline functions, which is used in the equation to calculate the dilution factor. Therefore, with the larger difference in streamline functions, the initial dilution factor will be greater than the cases that have a larger x_0 value. Furthermore, there seems to be a correlation in the rate of decrease in dilution factor with the two cases that had a smaller x_0 value. For Cases 1C and 1D, the dilution factors decreased at a much faster rate than the other two cases. The lower streamline angle is almost double in Case 1D

compared to Case 1A, while the upper streamline angle is less influenced by the decrease in the x_0 value. The increase in the streamline angle creates a much higher difference in streamline functions. The streamline angle is much more influenced by any change in source geometry whenever x_0 has been reduced. This is because the streamlines are more curved at a shorter distance. The farther the source is from the pumping well, the more horizontal the streamlines become, creating a smaller impact on θ_i with any change in geometry of the source.

Case 2 – Variable Source Zone Orientation and Fixed Symmetry

The results for Case 2 indicate that the source angle has a significant impact on the dilution factor calculation when comparing with a symmetrical and asymmetrical source. For Case 2A and Case 2B, the difference in the dilution factor is distinct, and begins to increase as the source angle decreases. The reason for the difference in dilution factor values is the streamline function angles are smaller with an asymmetrical source. This creates a lower difference in streamline functions, and subsequently leads to a lower dilution factor for Case 2B. The interesting part of the results is the differences between the curves increase with smaller angles, where the larger differences between the curves occur around 56.25°, 45°, 33.75°, and 22.5°. For these angles, the symmetrical source results in higher y-values than the asymmetrical source. Case 3D does not converge to zero because the source length is equal to the x_0 value. The streamline angle in the negative *y*-direction becomes larger as the source is rotated, which will not allow the dilution factor to decrease at the same rate as the previous

cases. Therefore, it is important for the x_0 value to be greater than the source length in order to have a smaller dilution factor if the source angle is small.

Case 3 – Variable Source Zone Length and Fixed Symmetry and Orientation

The final analytical case investigates the impact the source length has on the dilution factor. The source length is reduced by 10% for each step, and then divided by the maximum length. As the $\frac{y}{x_0}$ ratio begins to increase, the dilution factor correspondingly increases along with it. Changing the angle to 45° in Cases 3B and 3D creates smaller dilution factor values for larger length sources compared to Cases 3A and 3C. This is because compared to their perpendicular source counterparts the streamline angles have been reduced. For the curves with similar x_0 distances, the curves begin to converge with each other as the length of the line source diminishes. This is because when the source is smaller, the streamlines will become more horizontal. As the streamlines become more horizontal, the source angle has less of an impact on the dilution factor. The curves also appear to become less linear when the source length is larger.

Case 4 – Time Step Function

After analyzing the results for Case 4, one important takeaway from the dilution factor values is that when the source is a step function source, the difference between the integration methods indicates no estimated error. This indicates that both integration methods will suffice when doing the calculation. With the step function being equal to one if t is less than a, this makes for a straightforward calculation for the integration. The dilution factor for 18 days $\leq t \leq$ 34 days is equal to 0.346 because the source is

treated as constant during this time. Since the source is removed after 20 days, it will take 14 days after this time for the source to begin to decrease. After this time, the source will decrease until the last contaminant particle has reached the well.

Case 5 – Exponential Decay Function

Changing the source type for the experiment was thought to have an impact on the dilution factor calculation before this study was done. In Case 5, the model uses the exponential decay function, as compared to the constant source in Case 4. The dilution factor values are very similar between these two cases for $t = 20$ days, but as the time measurement increases, dilution factor values in the well for Case 5 begin to decrease. This is because the exponential decay source is breaking down and resulting in a smaller C_w at the extraction well. Depending on what the decay constant is for the source, this will have an impact on how much the dilution factor will decrease. The greater the time measurement, the more influence the decay constant will have on the dilution factor because the source has more time to breakdown. The Gaussian Kronrod method seemed to display the most consistent results, and therefore is the better model in this case.

Case 6 – Leaking Source Function

The final case has similar results to Case 5. The results show that the source type used in the model impacts the dilution factor. The Gaussian source type dilution factor generally decreases as the time measurement increases, depending on the standard deviation value. For $\sigma = 30$ days, the dilution factor did not decrease until after $t = 40$ days. The reason for this is that the bigger standard deviation creates larger concentrations for longer periods of time, so it takes more time to see a significant

impact on the dilution factor. It can be concluded that the larger the standard deviation, the longer it takes for the dilution factor to begin to decrease.

Since these functions are altered by different variables, it makes it difficult to do a comparison because each variable can have a different impact on that specific function. For Case 5 and Case 6, depending on what value is used for the decay constant and the standard deviation, this can either make the results very similar, or create a small difference between the two. Based on this particular scenario, the values are comparatively similar, because as the time measurement increases, both source types show a decrease in dilution factor. Altering a few of the initial parameters can change the dilution factor significantly. The percent difference between the two integration methods in Case 5 were higher than Case 6 for smaller time measurements. The difference between integration methods became larger in Case 6 as the time measurements increased, but still remained smaller than Case 5.

DISCUSSION

The results in this thesis are applicable to many different issues dealing with environmental remediation. The first thing is that it can enlighten us about the source that we are investigating. One can make a proper assessment of the dilution factor by knowing some of the variables that are used in the calculation, such as the aquifer thickness, regional flow q_0, the distance from the source to the pumping well x_0, and the length of the source. Knowing a few of these measurements and the dilution factor can help determine the orientation of the source, the geometric shape of the source, and the type of source, given that these parameters are accurate. This can save an environmental agency or organization a considerable amount of time by understanding the source better, and can create a shorter time to plan for the project. The longer it takes to clean up a remediation site, the more likely that the source will be increasingly difficult to completely remove and it could extend the project timeframe if not done correctly.

Another reason this project is unique and useful is that it provides a quantitative connection between the equations, and what is actually happening in the subsurface. This is extremely valuable because it provides an answer to why the results you see in an extraction well are behaving the way that they are. The concentration seen at a pumping well can give immediate insight for some other important properties of the source. By using concentrations seen in the pumping well, one could compare the results to the curves generated in this thesis to be able to find the orientation of the contaminant source. Understanding the geometric factors contributing to the calculation of the dilution factor is crucial to setting up a remediation project. Placing an extraction well

with a small source angle and an asymmetrical source relative to the x-axis is the optimal position in order to dilute the source as much as possible, because it will result in the lowest dilution factor. A lower pumping rate is desired in order prevent drawdown, and also allow for a cheaper, more efficient cleanup process. If the source is asymmetrical, this may require higher pumping rates. Higher pumping rates may pose the need for more robust equipment, and therefore increase the expenses of the project. This is something that needs to be assessed by the individual responsible for the cleanup, and dealt with according to their budget and the timeframe of the project.

Providing a first screening to a specific project is one of the many uses that this project can provide. It is vital for a company or private consultant to be able to assess the situation and be able to come up with a fast quantitative solution to the issue. Afterwards, a more powerful and precise numerical model can be produced if desired. Creating a numerical model takes time, and oftentimes will have many errors associated with it. Because of these errors, it is extremely important to have an analytical model to compare the numerical results to in order to know whether the results are correct. Numerical models are useless if they do not have an analytical model to compare the results against. The quantitative solution this model creates allows for a numerical model to be performed with confidence.

Awareness issues are one of the main reasons why this thesis was developed. A common misconception is that people believe once the source reaches the extraction well, the C_w should be equal to the C_0. We know this is not the case, because the capture zone extends beyond the line source for some values of Q and source geometry. This

area within the aquifer contains freshwater, and therefore will dilute the concentration seen at the pumping well. Many companies start out with creating a numerical model for the cleanup, which can be very useful, but isn't always necessary. One of the many goals of this thesis was to provide an understanding and awareness that analytical models are still very useful and can oftentimes be the better option because they require less input parameters.

All of these cases will display a different result; each situation trying to depict a unique scenario to see which geometric factor is the most influential in calculating the dilution factor. Because this model is only investigating advection of the source moving throughout the aquifer and neglects both dispersion and diffusion, it is meant to be a guideline for calculating the dilution factor during a remediation cleanup project. Other assumptions that could impact the dilution factor results are that it is a confined aquifer, and it is horizontally isotropic. For this particular scenario, the pumping rate is small enough that it would not have a significant impact on the dilution factor if the aquifer were unconfined. Pumping rates used in this model create a small cone of depression, so the aquifer can be treated as a constant thickness. For anisotropy, the results would change depending on how the hydraulic conductivity distributed throughout the aquifer. This could create different travel times for the contaminant particles, consequently changing the dilution factor for different time measurements. Depending upon the source geometric orientation and source type, the individuals responsible for the site project can use these models as a reference to develop the cheapest, most effective remediation process possible.

FUTURE WORK

This thesis only concerns a single well capture zone. For future work, it would be beneficial to expand the work to multiple well capture zones such as double-well, triple-well design. Providing work analysis for multiple well capture zones will provide more insight on what proper remediation technique should be utilized. Expanding upon the different source types using the modified travel-time equation would be useful to confirm how much of an impact source types has on the dilution factor.

The approach used in this thesis generally cannot be applied to deal with dispersion, which may play a secondary effect in influencing the dilution factor. My rationale of saying so is because the system investigated is an advection-dominating process because the pumping well is often positioned near the source zone. Dispersion may result in a few consequences that can be briefly illustrated as follows. Firstly, dispersion will somewhat expand the sizes of the contaminated source and contamination plume; such an effect may lead to a somewhat larger dilution factor in the pumping well. Secondly, the dispersion will lead to an earlier arrival time of the contaminant to the pumping well. Nevertheless, one has to call a numerical simulation to deal with advection and dispersion processes under a pump-and-treat scenario, which is outside the scope of this study.

Several studies have been done on the three-dimensional (3D) behavior of contaminants flowing through an aquifer (Clement et al., 1998; Mao et al., 2006; McDonald and Harbaugh, 1988). It would be interesting and worthwhile to investigate the impact a 3D source shape will have on the dilution factor calculation. The expected

results should be similar to the 2D results done in this thesis, only more precise since it is able to more accurately depict the shape of the source. It would also be helpful to perform some of these experiments for specific geologic settings to help verify some of these results. Simulating different source shapes and types could provide tangible evidence as to how the dilution factor behaves in specific areas. The results could then be compared to this model, and can verify the results shown in this thesis.

Future work could also entail trying to investigate how varying lithology influences the dilution factor. An important question is if these results are comparable with different geologic media, and how much the porosity and permeability of lithology play a governing role in the dilution factor calculation. Bernstein et al. (2007) explored the impacts of dilution with a highly heterogeneous reservoir. This study suggests that reservoirs with low-permeability but are highly fractured are poorly misunderstood, and the exclusion of the dispersive mass flux between the well and the tracer produces errors in the calculation of the Darcy velocity. Development of analytical solutions that are capable of mitigating these errors associated with reservoir heterogeneity would be a very valuable addition to the scientific community.

CONCLUSION

The dilution factor for a remediation project is driven by multiple factors. The orientation, along with the symmetry of the source, both have a significant impact on the dilution factor calculation. The results in Case 1 show that as the $\frac{\Delta y}{L}$ increases, the dilution factor decreases. This indicates that as the source becomes more asymmetrical, the dilution factor decreases. The reason for this phenomenon is that the area beyond the contaminant zone that is still within the capture zone becomes larger as the source becomes more asymmetrical. A larger uncontaminated zone means there will be more dilution of the source. Symmetrical sources, or a shorter distance from the source the extraction can cause an increase in the dilution factor. The x_0 value seemed to create the highest dilution factor values and can be concluded as the most influential factor in this particular scenario. The *x*-values for the endpoints of the source also play a governing role in the dilution factor calculation. Case 2 indicated that the source angle has an impact on the dilution factor, causing a decrease as the source angle decreases. In Cases 2C and 2D, the values begin to differentiate more than Cases 2A and 2B. The angles where these cases were distinctly different were for lower source angles at 56.25°, 45°, 33.75°, and 22.5°. The reason for the differences is that whenever the x_0 value is reduced, the streamline angles are increased. The sum of the streamline angles is higher for the symmetrical source, and therefore creates a higher dilution factor. In Case 2D, the length of the line source is equal to x_0. Consequently, this never allows the streamline angle below the *x*-axis to decrease. Therefore, the curve for this case does not converge to zero like the previous cases. Case 3 shows the results for comparing the

dilution factor and the $\frac{y}{x_0}$ ratio. Case 3A has a slightly smaller dilution factor than Case 3D, because the x_0 in Case 3D is half of what it is in Case 3A. The results show that the dilution factor decreases as the length of the line source is decreased. The curves tend to look more linear as the source length decreases. This is because the streamlines are becoming more horizontal as the source decreases. Once the length is reduced enough, the curves tend to merge together, even if the source angle is different.

Cases 4, 5 and 6 allow us to calculate the dilution factor after implementing a time dependent source type. The results show that for the values used, the dilution factors were fairly similar for all three of the source types for early time measurements. As the time measurement increased, the dilution factor began to decrease for Case 4, 5 and 6. Depending on the variables for each source type, the rate the dilution factor decreased changed. Case 4 was treated as a constant concentration until the source was removed. Once the last contaminants began reaching the well, the C_w value begins to decrease. The C_w value rapidly decreases at the beginning and then slowly approaches zero over the 4-day interval. For Case 5, the dilution factor was highest with the lowest decay constant and small time measurement, and in Case 6 the dilution factor was highest when the standard deviation was the largest and the time measurement was small. Two different integration methods were performed for each model to see how the values compared to one another. For Case 5, the dilution factor was higher with a larger decay constant with the Gaussian Quadrature method, while the opposite result occurred with the Gaussian Kronrod method for t = 20 days and t = 40 days. Both methods showed increasing dilution factors for lower decay constants during t = 60 days. During

Case 6, the dilution factor increases with the higher standard deviation values for both integration methods, but the values are limited by the time measurement.

Based on results, it can be concluded that minimizing the angle of the source, keeping the extraction well a farther distance from the source, and making the source asymmetrical relative to the *x*-axis will lower the dilution factor values. While making the source asymmetrical lowers the dilution factor, this also requires a higher pumping rate. This can lead to over-pumping and aquifer drawdown if not regulated properly. The x_0 value had the most influence on the dilution factor because of the change in streamline angles and theoretically more or less freshwater to help dilute the source.

The results for the integrations in Case 4, 5, and 6 were difficult to compare. Since different variables were used for the different source types, quantifying the results and comparing between the three cases proved impractical. The source type has more influence on the dilution factors as the time measurement increases. In Case 5, the Gaussian Kronrod integration method seemed to be the more accurate method. Deriving this equation is beneficial, and these equations can be retrofitted for any source type in MATLAB.

This project is meant to represent 2D scenarios, and is only meant to be a guideline for the first screening of remediation projects. The variables will change in a case-by-case fashion, and may not be as accurate for heterogeneous and complex reservoirs. Creating the most accurate, and efficient models is always something pursued throughout the academic community, and with this additional information, an

individual can quickly assess a groundwater contamination scenario with confidence before investing more time and money into a project.

REFERENCES CITED

Bair, E. S., and Lahm, T. D., 1996, Variations in Capture-Zone Geometry of a Partially Penetrating Pumping Well in an Unconfined Aquifer: Ground Water, v. 34, no. 5, p. 842-852.

Bair, E. S., Springer, A. E., and Roadcap, G. S., 1991, Delineation of Traveltime-Related Capture Areas of Wells Using Analytical Flow Models and Particle-Tracking Analysis: Ground Water, v. 29, no. 3, p. 387-397.

Bear, J., and Jacobs, M., 1965, On the Movement of Water Bodies Injected Into Aquifers: Journal of Hydrology, v. 3, no. 1, p. 37-57.

Bernstein, A., Adar, E., Yakirevich, A., and Nativ, R., 2007, Dilution Tests in a Low-Permeability Fractured Aquifer: Matrix Diffusion Effect: Ground Water, v. 45, no. 2, p. 235-241.

Calvetti, D., Golub, G., Gragg, W., and Reichel, L., 2000, Computation of Gauss-Kronrod Quadrature Rules: Mathematics of Computation of the American Mathematical Society, v. 69, no. 231, p. 1035-1052.

Chen, L., and Knox, R., 1997, Using Vertical Circulation Wells for Partitioning Tracer Tests and Remediation of DNAPLs: Groundwater Monitoring & Remediation, v. 17, no. 3, p. 161-168.

Christ, J. A., and Goltz, M. N., 2002, Hydraulic Containment: Analytical and Semi-Analytical Models for Capture Zone Curve Delineation: Journal of Hydrology, v. 262, no. 1–4, p. 224-244.

Clement, T., Sun, Y., Hooker, B., and Petersen, J., 1998, Modeling Multispecies Reactive Transport in Ground Water: Groundwater Monitoring & Remediation, v. 18, no. 2, p. 79-92.

Cohen, R. M., Mercer, J. W., Greenwald, R. M., and Beljin, M. S., 1997, Design Guidelines for Conventional Pump-and-Treat Tystems, United States Environmental Protection Agency, Office of Research and Development, Office of Solid Waste and Emergency Response.

Cunningham, J. A., Hoelen, T. P., Hopkins, G. D., Lebrón, C. A., and Martin, R., 2004, Hydraulics of Recirculating Well Pairs for Ground Water Remediation: Ground Water, v. 42, no. 6/7, p. 880.

Eckhardt, D. A., and Oaksford, E. T., 1988, Relation of Land Use to Ground-Water Quality in the Upper Glacial Aquifer, Long Island, New York: Geological Survey-Water Supply Paper (USA).

Fetter, C. W., 1999, Contaminant Hydrogeology: Prentice-Hall, Upper Saddle River (NJ, USA), v. 2nd ed.

Güven, O., Falta, R., Molz, F., and Melville, J., 1986, A Simplified Analysis of Two-Well Tracer Tests in Stratified Aquifers: Ground Water, v. 24, no. 1, p. 63-71.

Hoopes, J. A., and Harleman, D. R., 1965, Wastewater Recharge and Dispersion in Porous Media: Journal of the Hydraulics Division, v. 93, no. 5, p. 51-72.

-, 1967, Dispersion in Radial Flow From a Recharge Well: Journal of Geophysical Research, v. 72, no. 14, p. 3595-3607.

Javandel, I., and Tsang, C.-F., 1986, Capture-Zone Type Curves: A Tool for Aquifer Cleanup: Ground Water, v. 24, no. 5, p. 616-625.

Kompani-Zare, M., Zhan, H., and Samani, N., 2005, Analytical Study of Capture Zone of a Horizontal Well in a Confined Aquifer: Journal of Hydrology, v. 307, no. 1–4, p. 48-59.

Mao, X., Prommer, H., Barry, D. A., Langevin, C. D., Panteleit, B., and Li, L., 2006, Three-Dimensional Model for Multi-Component Reactive Transport with Variable Density Groundwater Flow: Environmental Modelling & Software, v. 21, no. 5, p. 615-628.

McDonald, M. G., and Harbaugh, A. W., 1988, A Modular Three-Dimensional Finite-Difference Ground-Water Flow Model: USGS-TWRI Book 6, Chapter A1. 1988.

Mieles, J., and Zhan, H., 2012, Analytical Solutions of One-Dimensional Multispecies Reactive Transport in a Permeable Reactive Barrier-Aquifer System: Journal of Contaminant Hydrology, v. 134, p. 54-68.

Miller, D. W., 1980, Waste-Disposal Effects on Ground Water: Premier Press. Berkeley, Calif.,(34941), p. 512.

Park, E., and Zhan, H., 2001, Analytical Solutions of Contaminant Transport from Finite One-, Two-, and Three-Dimensional Sources in a Finite-Thickness Aquifer: Journal of Contaminant Hydrology, v. 53, no. 1–2, p. 41-61.

Ptak, T., Piepenbrink, M., and Martac, E., 2004, Tracer Tests for the Investigation of Heterogeneous Porous Media and Stochastic Modelling of Flow and Transport—

a Review of Some Recent Developments: Journal of Hydrology, v. 294, no. 1–3, p. 122-163.

Shan, C., 1999, An Analytical Solution for the Capture Zone of Two Arbitrarily Located Wells: Journal of Hydrology, v. 222, no. 1–4, p. 123-128.

Steward, D. R., 1999, Three-Dimensional Analysis of the Capture of Contaminated Leachate by Fully Penetrating, Partially Penetrating, and Horizontal Wells: Water Resources Research, v. 35, no. 2, p. 461-468.

USGS, 2016, National Water Information System data available on the World Wide Web (Water Data for the Nation), accessed [November 10, 2016], at URL https://md.water.usgs.gov/faq/groundwater.html.

Wollenhaupt, N. C., Springman, R., and Doersch, R., 1990, Atrazine in Groundwater: A Current Perspective, University of Wisconsin-Extension, Cooperative Extension, College of Agricultural and Life Sciences, University of Wisconsin-Madison.

Zhan, H., 1999, Analytical Study of Capture Time to a Horizontal Well: Journal of Hydrology, v. 217, no. 1–2, p. 46-54.

Zhan, H., and Cao, J., 2000, Analytical and Semi-Analytical Solutions of Horizontal Well Capture Times Under No-Flow and Constant-Head Boundaries: Advances in Water Resources, v. 23, no. 8, p. 835-848.

Zhan, H., and Sun, D., 2007, Travel-Time Distribution from a Finite Line Contamination Source to an Extraction Well with Regional Flow: Advances in Water Resources, v. 30, no. 3, p. 389-398.

APPENDIX A

Derivation of the dilution factor equation for a constant concentration source

Q = pumping rate of the well [L^3/T]
q_0 = uniform regional flow specific discharge [L/T]
B = thickness of the confined aquifer [L]
x_0= distance from the center of the line source to the extraction well [L]
φ = streamline value passing through source [L^2/T]
y = y coordinate at an arbitrary point along the streamline [L]
y_0 = y coordinate at the source [L]
l = half length of the line source [L]
ω = decay constant [1/T]

Dimensionless terms:

$$\varphi_D = \frac{\varphi}{q_0 x_0} \quad , \tag{A1}$$

$$y_D = \frac{y}{x_0} \quad y_{0D} = \frac{y_0}{x_0} \ , \tag{A2}$$

$$l_D = \frac{l}{x_0} \ , \tag{A3}$$

$$Q_D = \frac{Q}{2\pi B x_0 q_0} \ , \tag{A4}$$

$$Q_{Dmin} = \frac{l_D}{\pi - \tan^{-1} l_D} \text{ . (Zhan and Sun (2007))} \tag{A5}$$

The equation used for determining the Q_{min} :

$$Q_{min} = Q_{Dmin}(2\pi B x_0 q_0) \ . \tag{A6}$$

Taking the dimensionless pumping rate (Q_D) and the dimensionless streamline function (φ_D) from the equations above, now the dilution factor (DF) can be solved.

To find DF, the difference in streamline functions, $|\varphi_1 - \varphi_2|$, needs to be calculated. This represents the flowrate per unit depth between these two streamlines. φ_1 and φ_2 represent the streamline values that pass through the upper and lower ends of the source. Applying the dimensionless variables into the equation, we now can generate a DF that is dimensionless.

$$DF = \frac{|\varphi_1 - \varphi_2|}{Q/B} = \frac{|\varphi_{1D} - \varphi_{2D}|}{2\pi Q_D} = \frac{\varphi_D}{\pi Q_D} \quad . \tag{A7}$$

Derivation dilution factor equation for time-dependent source concentration

For the derivation of the time-dependent dilution factor, first the dimensionless streamline function can be written as shown above in equation (A1). The variables y_D and y_{0D} are also defined above (A2). These are the *y*-coordinate at an arbitrary point along the streamline and the *y*-coordinate at the source, respectively. The equation can rewritten as the following equation:

$$\varphi_D = Q_D \tan^{-1} y_D + y_D \quad . \tag{A8}$$

The derivative of the dimensionless streamline function equation gives the following:

$$d\varphi_D = \left(\frac{Q_D}{1+y_D{}^2} + 1\right) dy_D \quad . \tag{A9}$$

The following travel-time equations are derived from Zhan and Sun (2007):

$$T(0) = 1 - Q_D \ln\left(1 + \frac{1}{Q_D}\right) \quad , \tag{A10}$$

$$T(0 \le y_D \le 1) = 1 - Q_D \ln\left[\frac{\sin\theta_f}{\sin\theta_i}\right] . \tag{A11}$$

One can now calculate the entering angle of a streamline to the extraction well (θ_f). The symbol θ_i represents the polar angle from the well to starting point at the source. Since θ_f is typically unknown, it is convenient to rewrite this value as:

$$\theta_f = \theta_i + \frac{2\pi q_0 B y}{Q} = \theta_i + \frac{y_D}{Q_D} \quad . \tag{A12}$$

To solve for θ_i, the following equation is applied:

$$\theta_i = \tan^{-1}\left(\frac{y}{x_0}\right) \quad , \tag{A13}$$

$$\sin\theta_i = \frac{y_D}{\sqrt{1+y_D{}^2}} \quad , \quad \cos\theta_i = \frac{1}{\sqrt{1+y_D{}^2}} \quad . \tag{A14}$$

Given the above equation (A12) to calculate θ_f, we can now write θ_f in the format needed to solve the equation involving *T*. A trig identity is used to simplify the equation below.

$$\sin\theta_f \;=\; \sin\left[\theta_i + \frac{y_D}{Q_D}\right] \;=\; \sin\theta_i \cos\left(\frac{y_D}{Q_D}\right) + \cos\theta_i \sin\left(\frac{y_D}{Q_D}\right) \;,$$

$$= \frac{y_D}{\sqrt{1+{y_D}^2}} \cos\left(\frac{y_D}{Q_D}\right) + \frac{1}{\sqrt{1+{y_D}^2}} \sin\left(\frac{y_D}{Q_D}\right) \;. \qquad \text{(A15)}$$

This can now be plugged back into the travel-time equation (A11) to solve for $T(y_D)$ and $T(l_D)$. The symbol l_D is considered to be the dimensionless full-length of the line source.

$$T(y_D) = 1 - Q_D \ln\left[\frac{y_D \cos\left(\frac{y_D}{Q_D}\right) + \sin\left(\frac{y_D}{Q_D}\right)}{y_D}\right] \;, \qquad \text{(A16)}$$

$$T(l_D) = 1 - Q_D \ln\left[\frac{y_{0D} \cos\left(\frac{l_D}{Q_D}\right) + \sin\left(\frac{l_D}{Q_D}\right)}{l_D}\right] \;. \qquad \text{(A17)}$$

Finally, the integral to solve for the concentration in the extraction well for the full length of the line source (l_D) is presented below. This equation combines equation (A9) with a time-dependent source function being integrated from 0 to l_D. The dilution factor (*DF*) can now be calculated using the equation (A19).

$$C_W = \frac{C_0}{\pi Q_D} \int_0^{l_D} f[t - T(y_D)] \left[\frac{Q_D}{1+{y_D}^2} + 1\right] dy_D \;, \qquad \text{(A18)}$$

$$DF = \frac{C_W}{C_0} \;. \qquad \text{(A19)}$$

APPENDIX B

MATLAB CODE

The MATLAB code for Case 5 and Case 6 is listed below. For each of these analytical solutions, there were two integration methods performed. The first was the Gaussian quadrature method.

Gaussian quadrature

For the Gaussian quadrature method, the function used to calculate the weights (w) and abscissas (x) is referenced in the Programs section of this thesis. The MATLAB function is named lgwt.m in the program.

The function is defined as: [x, w] = lgwt (n, a, b)

Where n is the number of nodes and [a, b] is the interval.

Once the desired number of nodes and interval is established, now the equation needs to be defined. The equation used for the exponential decay function in Case 5 is shown below. The values for the variables are t = 10 days, ω = 0.05 days^{-1}, and Q_D = 0.8.

```
f = exp(-(0.05*(10-(1-0.8*log(((x.*cos(x/0.8))+(sin(x/0.8)))/x))))).*((0.8./(1+(x.^2)))+1)
```

After this step, you can now multiply the weights times the function values calculated using the abscissas and sum the values together using the equation below.

```
value = sum (w.*f)
```

The new value can then be divided by πQ_D to get the dilution factor. Case 6 can be performed by replacing the function equation.

Gaussian Kronrod quadrature

For the next integration method, the function is already built into MATLAB.
The integration method used is called Gaussian Kronrod quadrature and the function name is quadgk.m in MATLAB. The walkthrough for how to use this function is listed below.

```
quadgk = (f, a, b, 'MaxInterval', n)
```

where f represents a function handle, [a, b] is the interval, and n is the number of nodes.

The code for Case 5 with t = 10 days, ω = 0.05 days^{-1}, and Q_D = 0.8 is listed below.

```
function [ f ] = expo(x)
% Geometric Source Control Case 5
% Exponential Decay source

f = exp(-(0.05*(10-(1-0.8*log(((x.*cos(x/0.8))+(sin(x/0.8)))/x))))).*((0.8./(1+(x.^2)))+1)

end
```

First a function handle needs to be set.
The function handle will be set using the function in Case 5 and will be represented by the variable "f."

```
f = @expo
```

Now the integration function can be used, where the interval is from 0 to l_D (l_D = 0.5).

```
quadgk = (f, 0, 0.5, 'MaxInterval', 40)
```

This value can now be divided by πQ_D to solve for the dilution factor.

APPENDIX C

MATLAB

Legendre-Gauss Quadrature Weights and Nodes

by Greg von Winckel

26 Feb 2004 (Updated 11 May 2004)

Computes the Legendre-Gauss weights and nodes for solving definite integral

https://www.mathworks.com/matlabcentral/fileexchange/4540-legendre-gauss-quadrature-weights-and-nodes?requestedDomain=www.mathworks.com